ChemInform Abstract: Structural Insight into the Aromatic Amino Acid Hydroxylases and Their Disease-Related Mutant Forms

ARTICLE *in* CHEMICAL REVIEWS · SEPTEMBER 1999

Impact Factor: 46.57 · DOI: 10.1021/cr980450y · Source: PubMed

2 AUTHORS, INCLUDING:

Torgeir Flatmark
University of Bergen
267 PUBLICATIONS **7,191** CITATIONS

Structural Insight into the Aromatic Amino Acid Hydroxylases and Their Disease-Related Mutant Forms

Torgeir Flatmark

Department of Biochemistry and Molecular Biology, University of Bergen, Årstadveien 19, N-5009 Bergen, Norway

Raymond C. Stevens*

Department of Molecular Biology, Institute for Childhood and Neglected Diseases, The Scripps Research Institute, 10550 North Torrey Pines Road, La Jolla, California 92037

Received January 21, 1999 (Revised Manuscript Received April 19, 1999)

Contents

1. Introduction

The mammalian aromatic amino acid hydroxylases (phenylalanine, tyrosine, and tryptophan hydroxylase (PheOH, TyrOH, TrpOH, respectively)) are functionally and structurally closely related enzymes (e.g. 65% sequence identity and 80% sequence homology in the catalytic domains)[1] (Figure 1). This family of enzymes shares a common catalytic mechanism, in which dioxygen is used by an active site containing a single, reduced iron atom to hydroxylate an unactivated aromatic substrate (i.e., monooxygenase activity), concomitant with a two-electron oxidation of tetrahydropterin cofactor to its quinonoid dihydropterin form (Figure 2).[2] The enzymes play an important role in mammalian metabolism: PheOH initiates the catabolism/detoxification of high levels of phenylalanine, while TyrOH and TrpOH catalyze the rate-limiting steps in the biosynthesis of the neurotransmitters/hormones dopamine/noradrenaline/adrenaline and serotonin, respectively. In 1959, Kaufman[3] related a deficiency in hPheOH to the genetic disease phenylketonuria (PKU), and more recently a deficiency in hTyrOH has been related to the genetic disease L-DOPA responsive dystonia[4] and juvenile parkinsonism.[5] Current research is close to linking TyrOH with bipolar affective disorder[6] and studying the relationship between DNA polymorphism of the TyrOH gene and schizophrenia[7] (see section 4). Reduced biosynthesis of L-DOPA by TyrOH as a result of progressive degeneration of dopaminergic neurons in the nigrostriatal pathway is characteristic of idiopathic parkinsonism (Parkinson's disease), and evidence has recently been presented that the TyrOH enzyme system itself may contribute to the oxidative stress considered to be responsible for the neurodegeneration.[8] While the enzymes operate on different amino acid substrates, the similarity of substrate structure is apparent, and recent data have provided important sequence and mechanistic links between the different hydroxylases.

In solution, the aromatic amino acid hydroxylases form homotetramers with molecular mass ranging from 204 to 217 kDa. Sequence homologies, site-directed mutagenesis, and partial proteolysis experiments have demonstrated that these enzymes are composed of an N-terminal region (PheOH 1−142; TyrOH 1−155; TrpOH 1−177) with regulatory properties and a C-terminal region (PheOH 143−452; TyrOH 156−498; TrpOH 178−445) known to be

* Corresponding author.

10.1021/cr980450y CCC: $35.00
Published on Web 08/11/1999

Torgeir Flatmark, born in Norway in 1931, received his M.D. (1957) and Ph.D. (1995) from the University of Oslo for research carried out at the Nobel Medical Institute, Stockholm, with Hugo Theorell. He was a NIH International postdoctoral fellow (1965–67) in the chemistry department at the University of California at San Diego with Martin D. Kamen. He became an Associate Professor (1967) and later a Professor (1974) at the Department of Biochemistry and Molecular Biology, University of Bergen, Norway. He has been a visiting professor at the Institute of Enzyme Research, Madison (1977), Rockefeller University, NY (1983), and European Molecular Biology Laboratory, Heidelberg (1990). Flatmark has contributed to the fields of mitochondrial cytochromes, bioenergetics (nonshivering thermogenesis), and biogenesis as well as the structure and function of catecholamine storage vesicles and peroxisomes. A long-term interest involves studies on enzyme structure and function, including non-heme Fe- and Cu-dependent monooxygenases and vacuolar proton-ATPase related to the biosynthesis, storage, and release of catecholamines as neurotransmitters and hormones. The research on metalloenzymes includes phenylalanine hydroxylase, tyrosine hydroxylase, and dopamine β-hydroxylase and their disease-related mutant forms.

Raymond Stevens, born in Maine in 1963, received his B.S. (1986) from the University of Southern Maine and Ph.D. (1988) from the University of Southern California with Professor Robert Bau. He was an NIH postdoctoral fellow (1989–1992) in the chemistry department at Harvard University with Professor William Lipscomb. In 1992, Stevens started as an Assistant Professor of Chemistry at the University of California, Berkeley, with a joint appointment in neurobiology. In 1999, he accepted a full chaired professorship in Molecular Biology at The Scripps Research Institute in La Jolla, CA. Stevens has contributed to the fields of structural neurobiology (enzymes that synthesize neurotransmitters, receptors that bind neurotransmitters, toxins that modulate neurotransmitter signaling, and synthetic neuron design) and the field of antibody evolution/maturation and antibody-based catalysis. He has received a range of awards including the prestigious NSF Presidential Young Investigator Award and the Beckman Young Investigator Award.

involved in catalysis.[9] The C-terminal region of PheOH and TyrOH possess the same catalytic activity as the whole protein, and mutations associated with defects in this family of enzymes map predominantly to this region. The C-terminal domain can be further divided into the catalytic domain and tetramerization domain. The latter domain is typically the last 20−23 amino acids of the particular enzyme and is responsible for the oligomeric state of the enzyme forming a domain-swapped tetrameric coiled-coil.[10,11]

There has recently been a dramatic increase in the amount of structural information in this family of enzymes (Table 1). The crystal structures have been determined for human PheOH catalytic domain,[12] human PheOH catalytic domain plus tetramerization domain,[11] rat PheOH regulatory domain plus catalytic domain in the phosphorylated and unphosphorylated states,[13] human PheOH catalytic domain plus catechol inhibitors,[14] rat TyrOH catalytic and tetramerization domain,[10] and rat TyrOH catalytic domain and tetramerization domain in the presence of the pterin cofactor.[15] The crystal structures of the two hydroxylases have provided new and valuable information on their active-site structure, their binding of substrate and inhibitors and regulatory properties, as well as on the molecular basis of the diseases they cause when mutated. Here we review the structural data and discuss similarities and differences that are observed between the structures of PheOH and TyrOH as well as their potential significance to explain differences in substrate specificity and regulatory properties of the enzymes.

2. Phenylalanine Hydroxylase

The hydroxylation of L-phenylalanine to form L-tyrosine is the rate-limiting step in the catabolic pathway leading to the complete oxidation of L-phenylalanine (L-Phe) to carbon dioxide and water.[16] The reaction is catalyzed by the mononuclear non-heme iron enzyme phenylalanine hydroxylase (PheOH, phenylalanine 4-monooxygenase, EC 1.14.16.1) in the presence of the cofactor 6(*R*)-L-*erythro*-5,6,7,8-tetrahydrobiopterin (BH_4) and dioxygen. In the reaction the cofactor is oxidized to quinonoid dihydrobiopterin (qBH_2), which is regenerated to BH_4 by the NAD(P)H-dependent dihydropteridin reductase (Figure 2). Liver PheOH is a homotetrameric−homodimeric protein with a subunit mass near 50 kDa (50−53 kDa), and it has an absolute requirement for ferrous iron.[1] All of the mammalian PheOH enzymes whose sequences are known are highly homologous.

2.1. Overall Structure of the Human Enzyme

The aromatic amino acid hydroxylases are composed of three structural and functional domains: regulatory, catalytic, and tetramerization.[10−15] On the basis of the structures of the PheOH regulatory/catalytic domain and catalytic/tetramerization domain,[11−13] a full enzyme structure model can be assembled (Figure 3). The holoenzyme tetramer model has approximate dimensions of 85 Å × 100 Å

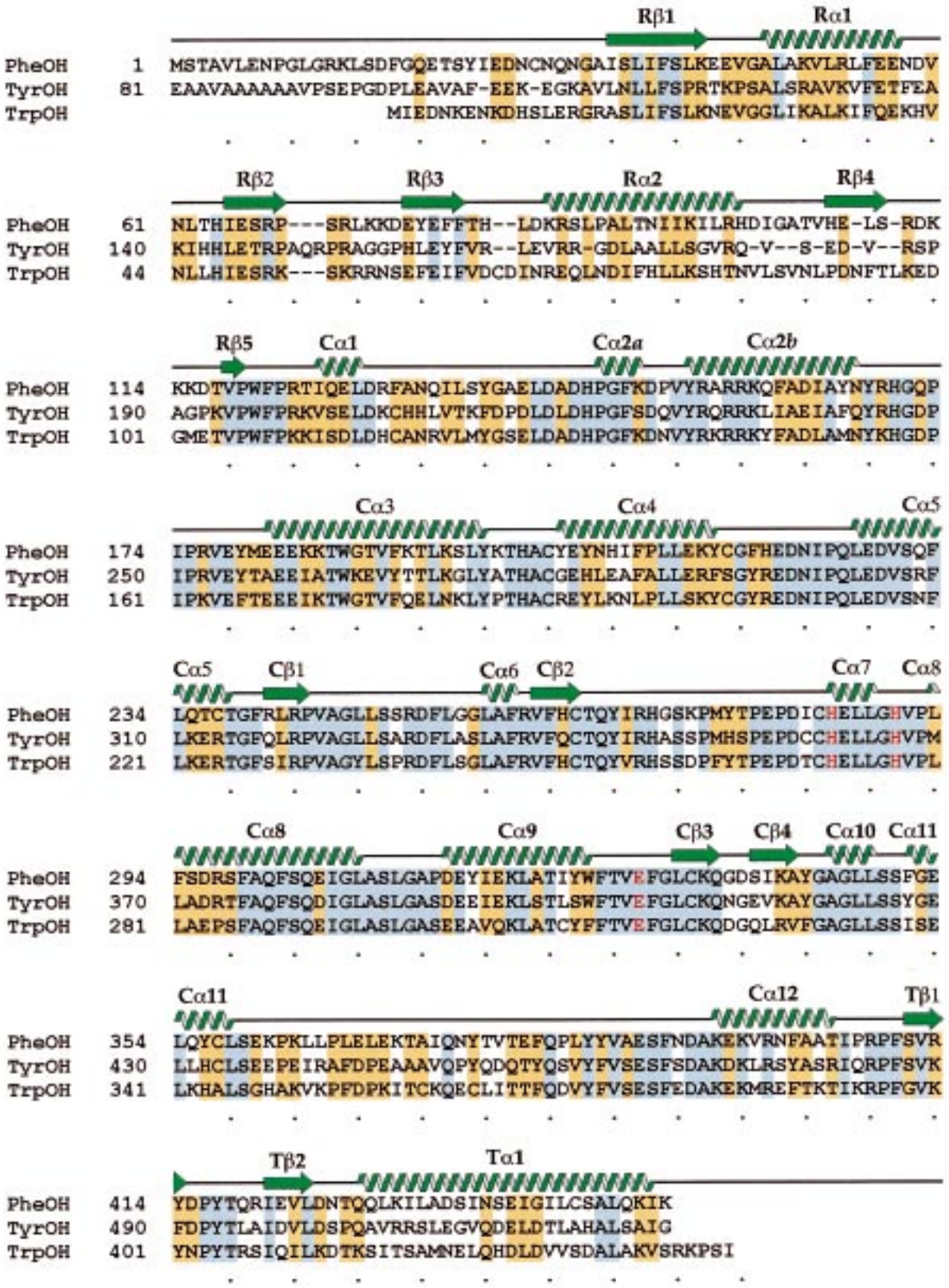

Figure 1. Sequence alignment of human PheOH (SWISS-PROT P00439), human TyrOH (SWISS−PROT P07101), and human TrpOH (SWISS−PROT P17752). Secondary structure assignment was determined from the coordinates of the combined PheOH structures with the program DSSP.[98] The secondary structure elements are indicated and numbered sequentially starting from the N-terminus. The residues identical in all three hydroxylases are colored blue; the residues identical in two of the hydroxylases are colored yellow. The three residues involved in iron binding are shown in red.

× 75 Å. The regulatory domain has a common α−β sandwich (βαββαβ) motif commonly observed for other regulatory domains. This domain is composed of a four-stranded antiparallel β-sheet flanked on one

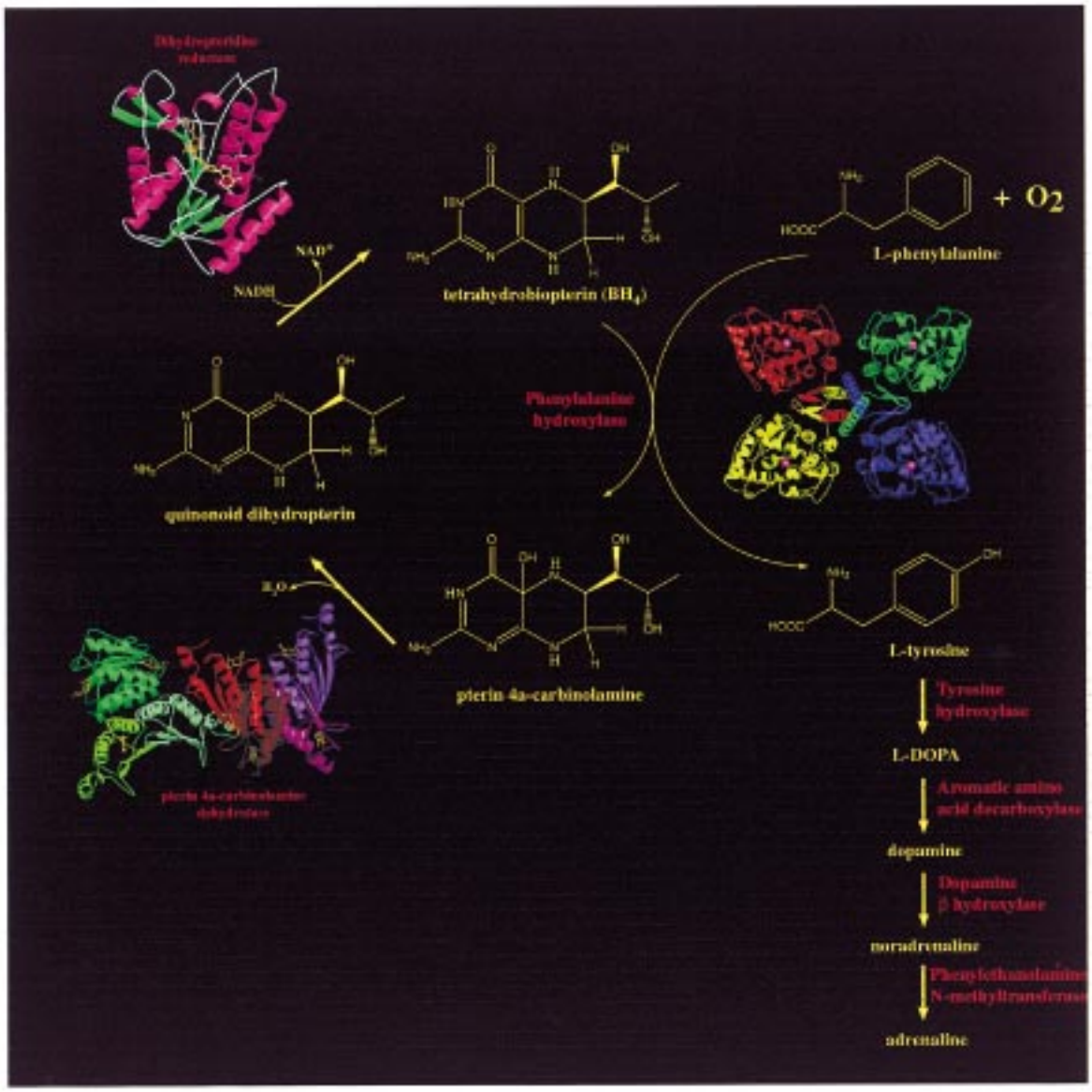

Figure 2. Reactions catalyzed by PheOH and TyrOH in which dioxygen is used by an active site containing a single, reduced iron atom to hydroxylate an unactivated aromatic substrate (L-phenylalanine/L-tyrosine), concomitant with a two-electron oxidation of tetrahydropterin cofactor (L-*erythro*-5,6,7,8-tetrahydrobiopterin, BH_4) to a 4a-hydrotetrahydropterin (4a-OH-BH_4 or 4a-Cyc-BH_4) intermediate. This intermediate is dehydrated to its quinonoid dihydropterin form (qBH_2) catalyzed by 4a-carbinolamine dehydratase,[53] and the tetrahydro form is regenerated by a NAD(P)H-dependent dihydropteridine reductase.[101]

Table 1. Crystal Structures of the Aromatic Amino Acid Hydroxylases in the Protein Data Bank (PDB)

structure (truncated forms)	resolution (Å)	PDB ID	ref
rTyrOH (ΔNH155)[a]	2.3	1TOH	10
rTyrOH (ΔNH155) with 7,8-dihydrobiopterin	2.3	2TOH	15
hPheOH (ΔNH117)	3.1	2PAH	11
hPheOH (ΔNH102 ΔCOOH428)	2.0	1PAH	12
hPheOH (ΔNH102 ΔCOOH428) with adrenaline inhibitor	2.0	3PAH	14
hPheOH (ΔNH102 ΔCOOH428) with nor-adrenaline inhibitor	2.0	4PAH	14
hPheOH (ΔNH102 ΔCOOH428) with dopamine inhibitor	2.1	5PAH	14
hPheOH (ΔNH102 ΔCOOH428) with L-DOPA inhibitor	2.15	6PAH	14
rPheOH(ΔCOOH430) Phosphorylated	2.2	1PH2	13
rPheOH(ΔCOOH430)	2.6	2PHM	13

[a] Δ indicates that region of the protein structure which was truncated (e.g., ΔNH155: residues 1−155 (regulatory domain) removed from the 498 residue rTyrOH).

side by two short α-helices and the other side by the catalytic domain. The catalytic domain is composed of 13 α-helices and 8 β-strands. The catalytic domain has a novel basket-like arrangement of helices and loops with an open active-site region that is approximately 13 Å × 13 Å wide and 10 Å deep. The tetramerization domain is composed of two antiparallel β-strands and a single 40 Å long C-terminal

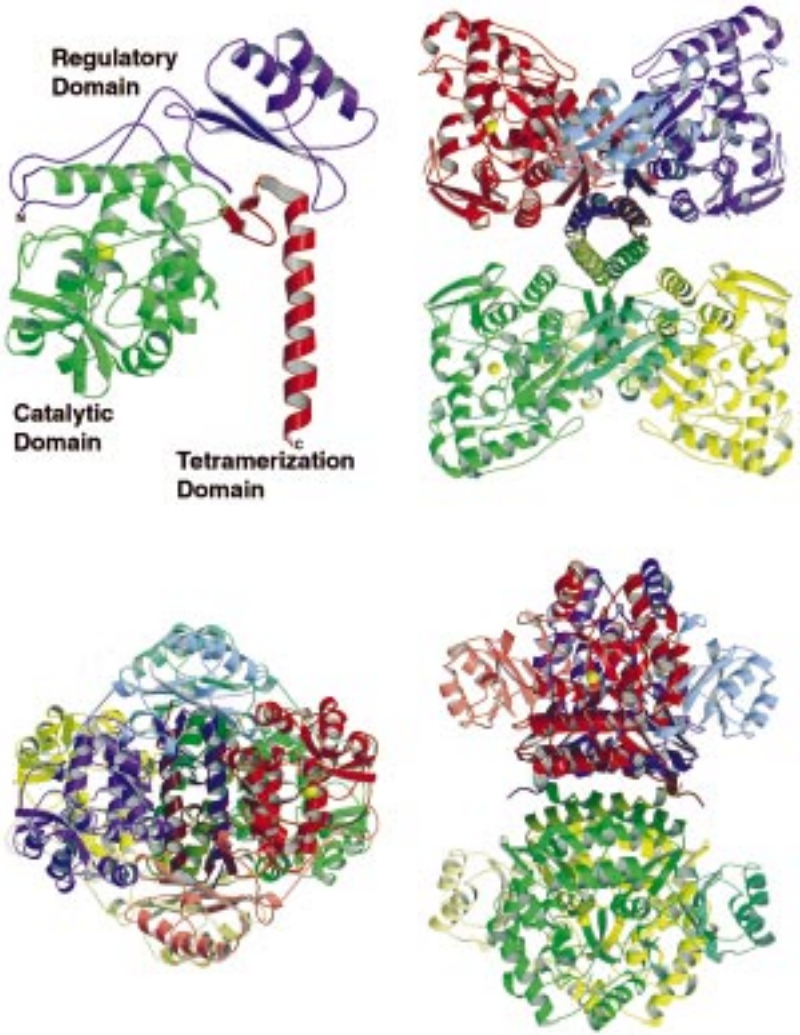

Figure 3. Model of the full-length human PheOH tetramer created by combining the structure of the regulatory/catalytic domain crystal structure and the catalytic/tetramer domain crystal structure. (top left) Monomeric form of full-length PheOH model with the regulatory domain (1−142) in purple, catalytic domain (143−410) in green, and tetramerization domain (411−452) in red. (top right) Tetramer view looking down the tetramerization domain. Each monomer is colored separately, with the lightest color representing the regulatory domain and darkest color representing the tetramerization domain. (bottom left) Side view 90° from view b. (bottom right) Alternative side view 90° away from views a and b. Of particular note is the location of the light-colored regulatory domains in close proximity to the neighboring catalytic domain for each dimer. The figures were produced by the programs Molscript[99] and Raster3D.[100]

α-helix which forms the domain-swapped coiled-coil core of the tetramer (Figure 3).

2.2. Catalytic Domain and Active Site

The structure of the hPheOH catalytic domain dimer[12] is shown in Figure 4 (top). The catalytic domain shows greater than 80% sequence identity between the hydroxylases (Figure 1). Each hPheOH monomer contains a total of 13 α-helices (45%) and 6 β-strands (16%), as determined by the secondary structure analysis program DSSP.[98] Approximate dimensions of the monomer are 50 Å × 45 Å × 45 Å, and the dimensions of the dimer are 85 Å × 45 Å × 45 Å.

The dimerization of the hPheOH monomers is mediated by the interaction of two symmetry-related loops (residues 414−420). A number of van der Waals contacts are observed, and 4 H-bonds are formed. Near the center of the 2-fold axis, the hydroxyl group of Tyr 417 hydrogen bonds to Gln 304 Nδ2 (3.2 Å). Away from the loop region, Nϵ1 of Arg 420 interacts with the side-chain and main-chain oxygen's of Thr 236 (3.1 and 3.3 Å). The two monomers interact across the dimerization interface with a buried surface area of 440 Å^2. A similar interface is observed in one of the interfaces of the tetrameric form of TyrOH (480 Å^2).

The recombinant truncated dimeric form of the enzyme used for the PheOH catalytic domain structural analysis in solution represents a fully activated state which does not demonstrate any cooperativity or measurable conformational change upon L-Phe binding.[17] Thus, the present structure represents the activated or *R* state of the enzyme. The active site consists of a 13 Å deep and 10 Å wide active-site pocket. Connected to the active site is a 16 Å long and 8 Å wide channel that may be where the substrate is directed into the active site. The majority of the 34 amino acids lining the active site are hydrophobic residues except for three charged glutam-

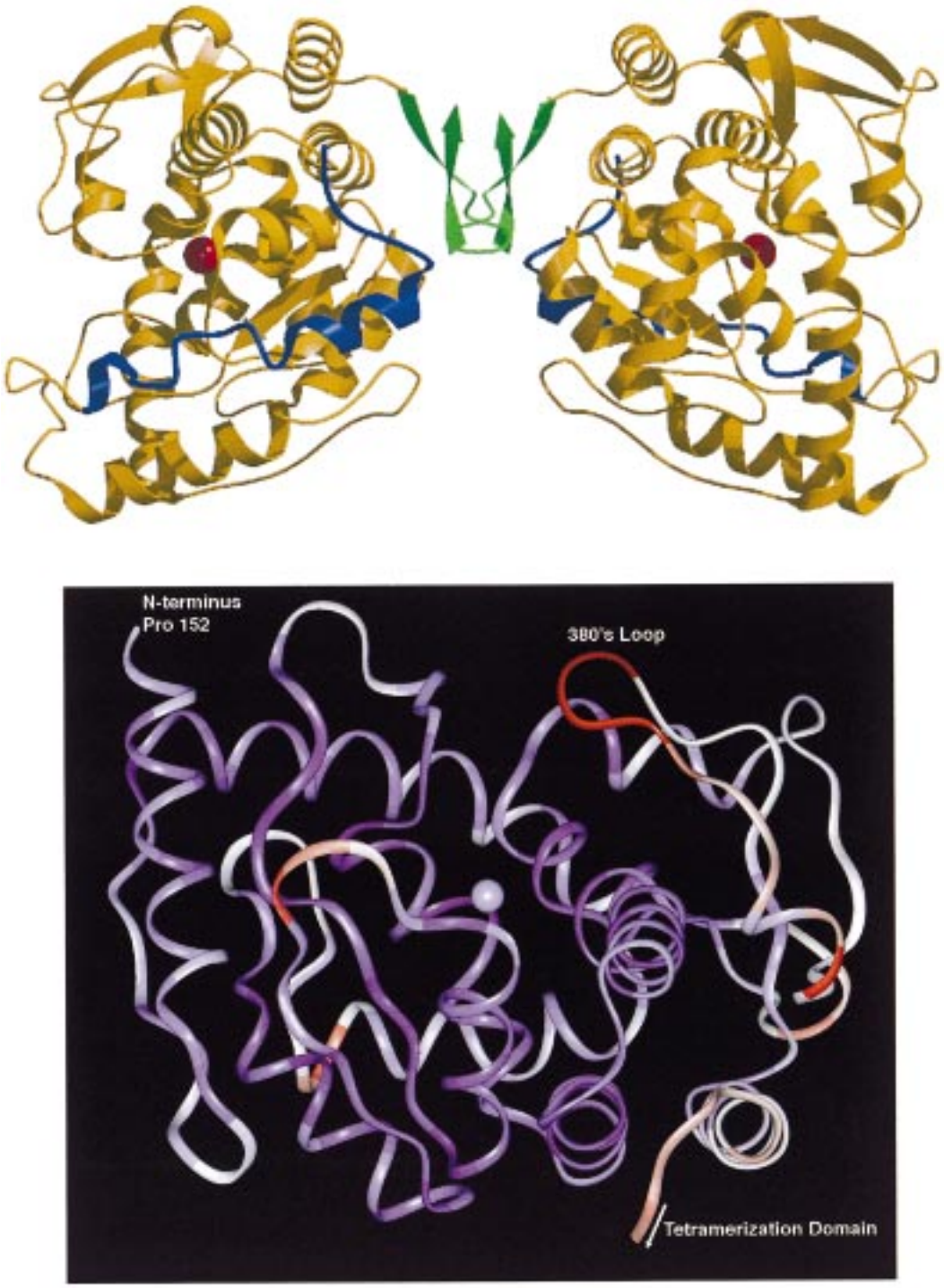

Figure 4. (top) Dimeric structure of human PheOH.[12] The C-terminal part of the regulatory domain (residues 117−142) is shown in blue, the catalytic domain (residues 143−410) in yellow, and the N-terminal part of the tetramerization domain (residues 411−424) in green. The iron atom in the active site is highlighted in red. (bottom) Cα diagram of PheOH with the atoms labeled according to B-factors. Red illustrates the residues of highest mobility (high B-factor); blue is the lowest mobility (low B-factor).

ic acids, two putatively charged histidines, and an uncharged tyrosine. Covering the entrance of the active site from the channel direction is a short loop (378−381) with some of the highest *B*-factors in the 2.0 Å structure (60−80 Å; Figure 4 (bottom)). The active site is very similar to that in rTyrOH[10] except that in rTyrOH the related loop (residues 427−429 in
rTyrOH versus 378−381 in hPheOH) is more rigid. As isolated, the recombinant hPheOH contains a high-spin form of Fe(III) iron ($S = {}^5/_2$) as in the rat enzyme.[18] In the 2.0 Å structure the iron atom is 10 Å below the surface of the protein on the "floor" of the active site at the intersection of the channel and the active-site pocket. The iron atom is coordinated to His 285 (N···Fe, 2.2 Å), His 290 (N···Fe, 2.2 Å), and one oxygen atom in Glu 330 (O···Fe, 2.1 Å) (Figure 5 (bottom left)). Both His 285 and His 290 have been shown by site-directed mutagenesis to be required for iron binding.[19] Well-defined electron

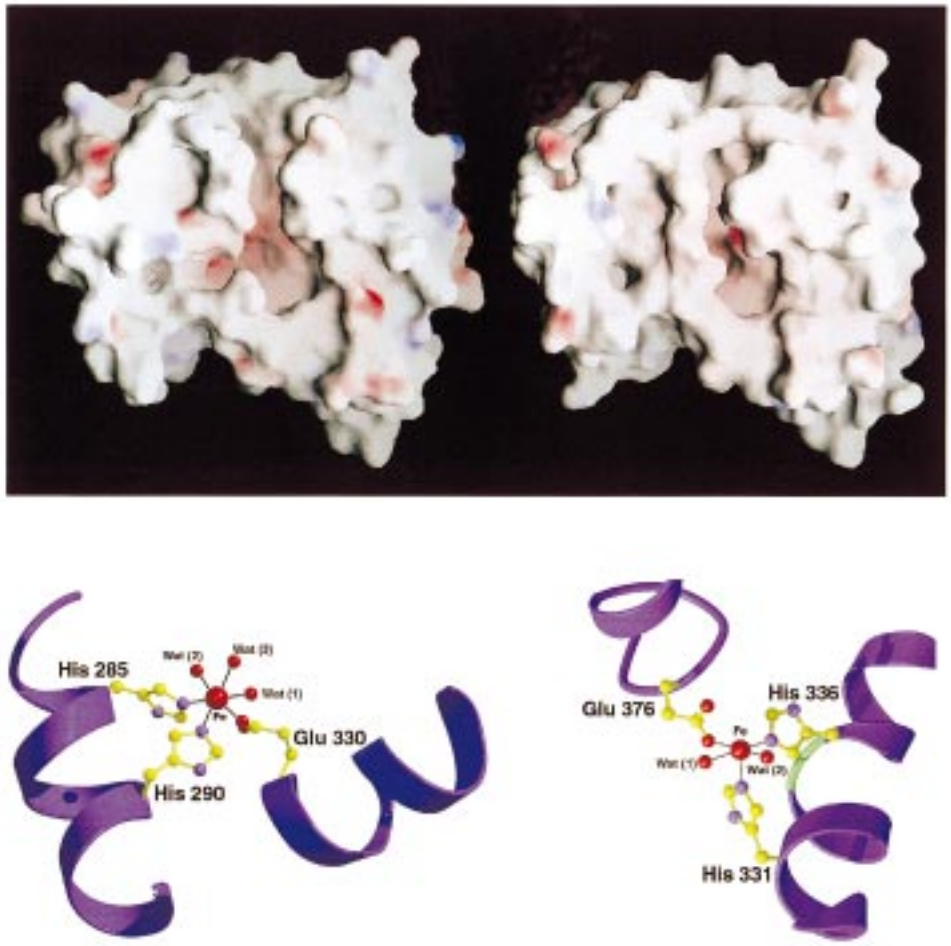

Figure 5. (top) GRASP surface of the catalytic domains of PheOH (left) and TyrOH (right) showing solvent access to the open active site. Charged regions are coded in red (negative) and blue (positive). (bottom) View of the iron binding site of PheOH and TyrOH with slightly different rotations to highlight the two active sites of one another. Helices involved in iron coordination are shown in blue. The green region in the TyrOH structure is a glycine residue which causes a kink in the helix, allowing the iron coordinating histidine residues to properly orient toward the iron atom.

density is also observed for three water molecules coordinated to the iron ($H_2O(1)\cdots$Fe, 2.3 Å; $H_2O(2)\cdots$Fe, 2.1 Å; $H_2O(3)\cdots$Fe, 2.3 Å). The iron ligands are arranged in an octahedral geometry, thus making the iron 6-coordinated as previously suggested based on spectroscopic evidence.[1] The observed temperature factors and bond lengths suggest that the axial water molecule (opposite His 285) is the most likely candidate for displacement. On the basis of proton NMR analysis, evidence has been presented that the binding of the substrate L-Phe and the inhibitor noradrenaline results in the displacement of a coordinated water molecule in rPheOH.[20] In contrast to hPheOH, only five ligands were reported in the structure of rTyrOH (Figure 5 (bottom right)).[10] However, spectroscopic results on hTyrOH have been interpreted as representing both 5- and 6-coordination of the iron atom,[21] whereas all data in hPheOH have consistently indicated that iron is 6-coordinated (see also section 3.1).[12]

To date, discussions on the catalytic mechanism of PheOH and TyrOH have been based on steady-state enzyme kinetic analyses including measurement of kinetic isotope effects and spectroscopic studies of the active-site iron without any definite information on the structure of the active site. In full agreement with the evidence presented so far,[1] the crystal structure has shown that the active site is very accessible to solvent and to the binding of exogenous ligands. Considering the hydrophobic nature and negative electrostatic potential of the active site (Figure 5 (top)), it will favor the binding of amphipathic molecules with a positively charged group. This is a general characteristic of the actual substrates, pterin cofactors, and inhibitors such as catecholamines. The more important question is how the specific interactions with the substrates and catechol inhibitors can be explained.

The hydroxylation reaction catalyzed by PheOH requires the presence of tetrahydrobiopterin (BH_4), dioxygen, and a redox-active ferrous iron before hydroxylation of L-Phe (Figure 2). In the structure the iron is located at the entrance of the pocket, thus leaving space for binding of both the pterin and the substrate. A motif of 27 amino acids (His 263 to His 289), which is highly conserved in the aromatic amino acid hydroxylases, has been proposed to be responsible for tetrahydrobiopterin binding.[9,22] Ten of the residues (Phe 263, Cys 265, Thr 266, Thr 278, Pro 279, Glu 280, Pro 281, His 285, Glu 286, and Gly 289) in this motif, including Glu 286 which was proposed to be of critical importance for pterin binding, are

present in the active site. In the structure Glu 286 is H-bonded to one of the coordinated water molecules ($H_2O(3)$) with a distance of 2.7 Å.[12,14] Recent proton NMR studies on the conformation of pterins bound at the active site of hTyrOH have revealed that the pterin is not coordinated to the metal.[23] For all the conformers of BH_2 and 6-MPH_4 examined by NMR of the binary complex, the estimated distance between either the 4-oxo atom in the pyrimidine ring or the N5 atom in the pyrazine ring and the metal was 3.3−4.1 Å. With respect to cofactor binding, Phe 254 is close to the iron (5.7 Å) and at the very edge of the putative pterin binding domain. The aromatic ring of Phe 254, which is completely conserved in the aromatic amino acid hydroxylases, may form a π-stacking interaction with the pterin ring as recently shown for the binary complex with rTyrOH (see section 3.2). Point mutations of Phe254 to leucine and alanine (in the truncated dimeric hPheOH, i.e., Gly103 to Gln428) have been found to increase (4-fold for F254L and 2-fold for F254A) the K_m value for the cofactor BH_4 (Bjørgo et al., unpublished data). The highly hydrophobic crevice structure with its negative electrostatic potential may explain why the enzyme cannot tolerate substitutions on the cofactor such as a carboxyl group in position 6 of the pyrazine ring and a hydroxy function at position 2 in the pyrimidine ring.[24] The open and solvent-accessible arrangement of the active-site pocket also explains why synthetic cofactors with bulky side chains in the 6 position can be accommodated together with the substrate in the catalytically-active ternary complex.[25] These factors also apply to catechol derivatives which function as high-affinity competitive inhibitors of BH_4 cofactor binding in hTyrOH.[26] The Fe(III) at the active site has been shown to directly coordinate to catecholamines (see section 2.3), and evidence has been presented that a residue with pK_a 5.1 is directly involved in the binding.[27]

Last, Tyr 325, which is in close proximity to the iron (Fe−OH, 4.5 Å) and highly conserved in the aromatic amino acid hydroxylases, should also be mentioned. The side chain of this residue is H-bonded (2.8 Å) to $H_2O(1)$ in Figure 5 (bottom) and has been considered to have a functional role in catalysis.[12] A similar spatial arrangement of a tyrosine in a non-heme iron active-site center has also been observed in the recent structure determination of the extradiol dioxygenase and is proposed to stabilize a radical intermediate in the catalytic cycle.[28] However, recent site-directed mutagenesis has revealed that a substitution of Tyr325 with Phe does not significantly change the catalytic properties of this dimeric truncated form except for a 3-fold increase in the K_m value for L-Phe of the enzyme (Bjørgo et al., unpublished data).

2.3. Binding of Catechol Inhibitors at the Active Site

In contrast to other mononuclear non-heme iron(II) enzymes,[29] there is no evidence that the substrates coordinate directly to the iron center of TyrOH and PheOH. Thus, proton NMR spectroscopic studies have clearly demonstrated that both L-Phe and BH_4 bind, as binary enzyme−substrate complexes, in close proximity to the active-site iron of hTyrOH, but in the second coordination sphere of the metal.[23,30] Kinetic studies suggest that BH_4 binds to rTyrOH first followed by O_2 and finally tyrosine,[31,32] but details of the common catalytic mechanism for the mononuclear non-heme iron aromatic amino acid hydroxylases remains to be determined (see section 3.5).[1] In contrast to the substrates, however, the catecholamine inhibitors (also common to these hydroxylases) directly coordinate to the metal center forming blue-green ligand-to-metal charge-transfer complexes as first described for hTyrOH.[33]

The molecular basis of the observed competitive type of inhibition by catecholamines (versus the pterin cofactor) of the PheOH- and TyrOH-catalyzed hydroxylation has been investigated using X-ray crystallography of the L-DOPA, dopamine, noradrenaline, and adrenaline binary complexes of a dimeric (and activated) truncated form (residues 117 to 424; "catalytic domain") of PheOH.[14] The catechol moiety in these structures clearly shows that the inhibitors bind to the iron center by a bidentate coordination of the two hydroxyl groups (distances of 2.0−2.1 Å; Figure 6 (top)), in agreement with the interpretation of the light absorption and resonance Raman spectroscopic data.[33] The same 2-His-1-carboxylate motif for the iron active site as in the ligand-free native structure was found, along with one water molecule. The four catecholamine−PheOH complexes are structurally identical, with no significant conformational differences. Their Cα atoms superimpose onto each other with an overall rmsd of only 0.08 Å (residues 117−424 used in the superimposition calculations). On the other hand, a slightly larger difference was observed when compared with the ligand-free native structure, where the catecholamine−PheOH complexes superimpose on the native structure with a rms displacement of 0.22 Å, implying a minor conformational change on ligand binding. The replacement of two water molecules with hydroxyl groups is compatible with previous EPR spectroscopic measurements on rat PheOH in which a change in the ligand field of the high-spin ($S = {}^5/_2$) Fe(III) changes from a rhombic symmetry (signal at $g = 4.3$) to a nearly axial type of EPR spectrum (signals at $g = 7.0$, 5.2, and 1.9).[18]

In addition to the bidentate coordination to the iron center, the catecholamines hydrogen bond with Glu330 and Tyr325 at the active site (distances of 2.6 Å between O2 and Tyr325 OH and Glu330 Oϵ2). These two residues may be involved in the stabilization of the relatively high-affinity binding ($[S]_{0.5} < 1\ \mu$M) of the amines at neutral pH.[27] The residues are highly conserved in the aromatic amino acid hydroxylases. Thus, according to the measured pH dependence for the dissociation of L-[^{3}H]-noradrenaline from the hydroxylases, a group with an apparent pK_a of 5.1 (at 20 °C) in rPheOH[27] and a pK_a of 5.3 (at 4 °C) in hTyrOH[34] has been found to be involved in the tight binding of the inhibitor at neutral pH. The closest protein residue to the catecholamine molecule which could satisfy the apparent pK_a value is Glu330. Protonation of Glu330 in PheOH at decreased pH

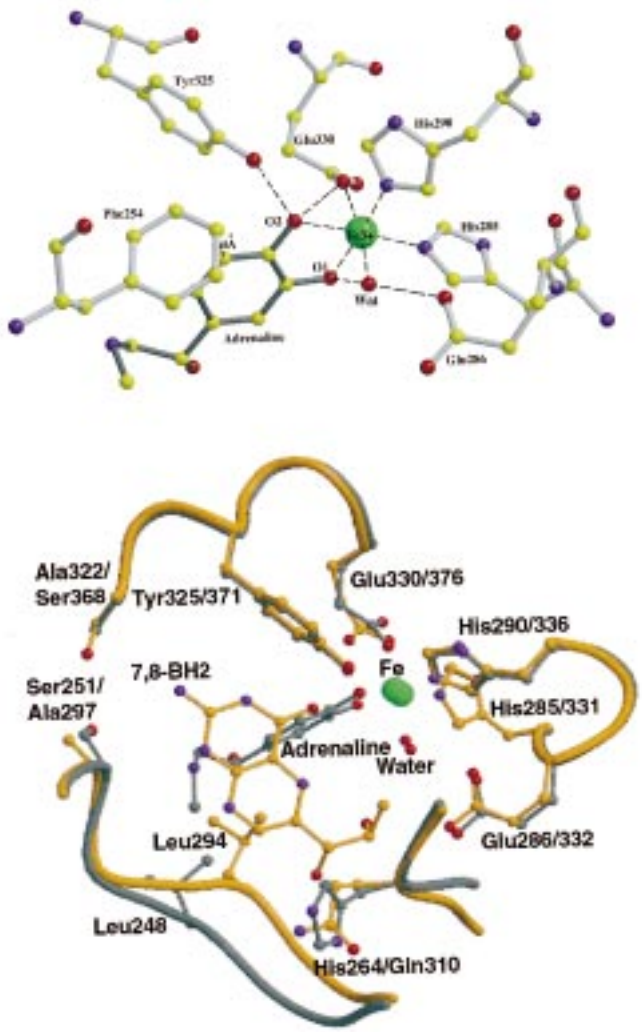

Figure 6. (top) Important active-site residues in the catechol−PheOH complexes as shown for the PheOH−adrenaline complex.[14] The catechol molecule is colored in dark gray and the ferric iron in green. (bottom) View of the active site of the PheOH−adrenaline complex (shown in gray) superimposed on the TyrOH−7,8-dihydrobiopterin complex (shown in orange).[14] The region of superimposition was chosen to be the Cα atoms of residues 281−319 (PheOH) and 327−365 (TyrOH) because this gave the best rms fit (0.34 Å). The individual oxygen atoms are shown in red, the nitrogen atoms in blue, and the iron atoms in green. The figures were produced by the programs Molscript[99] and Raster3D.[100]

could reverse the stabilizing effect that its carboxyl group has on the proton of the catecholic hydroxyl group.

Natural catecholamines such as dopamine, noradrenaline, and adrenaline are potent inhibitors of TyrOH and PheOH due to their tight binding to Fe(III) at the active site of the enzymes. Proton NMR and EPR spectroscopy have shown that the addition of stoichiometric amounts of dopamine to hTyrOH−Fe(II) results in an oxidation (by dioxygen?) of the iron to Fe(III) and the formation of the characteristic catecholamine-to-iron charge-transfer complex.[35] This complex represents a reversibly inactive form of the enzyme[26] in which the reduction of its ferric state by BH_4, and thereby generation of a catalytically competent form (oxidation level: Fe(II)) of the enzyme, is prevented. The same binding mode has been proposed for the catechol L-DOPA, the product of the TyrOH reaction, but its lower binding affinity than that of the catecholamines may be due to its sterically and electrostatically less favorable carboxyl side chain.[26] The crystal structure of the binary complex of tetrameric (and activated) truncated form (residues 164−498) of rTyrOH with the oxidized pterin cofactor (BH_2)[15] clearly demonstrates that the binding of the cofactor and the catecholamines at the active site overlap (Figure 6), as expected from the competitive type of inhibition of the respective enzyme activities by the amines.[26] The best superimposition for the active site residues was obtained with the Cα atoms between Pro281−Glu319 (hPheOH) and Pro327−Glu365 (rTyrOH). This region of the structure best illustrates the overlap for the catecholamine and the pterin binding sites in the two hydroxylases. The carbonyl oxygen in the C4 position on the pterin ring, as well as the C4a and C4 carbon atoms, overlap with the C5−C6 carbon atoms on the catecholamine inhibitor in the hPheOH structure. Most of the active-site residues are conserved in rTyrOH and hPheOH. The loop between hPheOH residues 245−250 (in rTyrOH 175−189) has the largest positional differences. In the rTyrOH−pterin structure, this is involved in binding the pterin (see section 3.2). There are hydrogen bonds between the carbonyl oxygen of the main chain and the N8 of BH_2. This loop packs close to another region (hPheOH residues 128−141) in which all out of 12 residues are different from rTyrOH. In the rTyrOH structure there was no electron density observed for this region (residues 178−186). Another important residue difference between the two hydroxylases is Gln310 in TyrOH which hydrogen bonds by its carbonyl oxygen to the C2′ hydroxyl group on the dihydroxypropyl side chain of BH_2 and is also stabilized by hydrogen bonds to Ser303 Oγ. In hPheOH, this residue is replaced by His264, which instead hydrogen bonds through one water molecule on each side to the carbonyl oxygens of residues Phe254 and Leu128. Two "structurally" conserved differences in the active-site residues are Ser251 in hPheOH, which is an Ala297 in rTyrOH, whereas Ala322 in hPheOH is a Ser368 in rTyrOH. Both these serines are between 3.7 and 3.9 Å away from the C2 amine in the pterin and about 2.8 Å away from each other.

The open and spacious active site together with the lack of protein contacts with the amine group of the catecholamines is consistent with the finding that both (*R*)- and (*S*)-adrenaline are equally effective in their inhibition for PheOH.[35b] Therefore, the majority of the binding strength comes from the ligand-to-metal charge-transfer interactions between the hydroxyl groups of the catecholamines and the iron. The essential requirement that seems to be of importance for inhibition is an intact catechol moiety (1,2-benzenediol). The crystal structures of the inhibitor complexes clearly show that the binding occurs only by the catechol moiety with charge-transfer interactions to the iron.

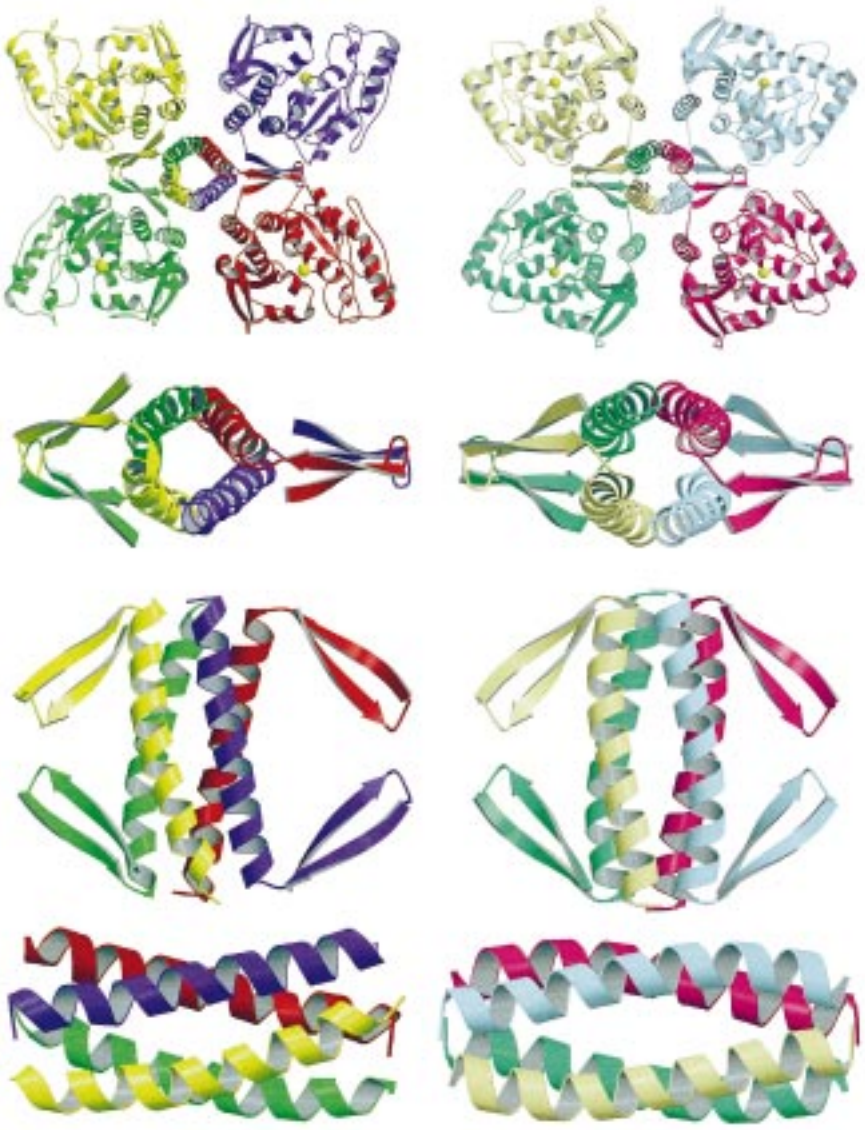

Figure 7. (top) Ribbon diagram representations of the $PheOH_{Cterm}$ (left) and $TyrOH_{Cterm}$ (right) tetramers. The four subunits are shown in different colors. In the PheOH tetramer, the 2-fold crystallographic axis relates subunits A (yellow) and B (purple) to C (green) and D (red), and the noncrystallographic 2-fold axis relates the dimer AC to BD. In the TyrOH tetramer, the four subunits are related by a crystallographic 222 symmetry. The coiled-coil motif is visible in the center of each tetramer. The iron bound in the active sites are shown as yellow spheres. Figure generated using the programs MOLSCRIPT[99] and RASTER3D.[100] (top middle) Tetramerization domain of PheOH (left) and TyrOH (right). The TyrOH tetramer structure can clearly be seen to be more symmetrical than the PheOH tetramer structure. (bottom middle) Ninety degree rotation of view b illustrating the asymmetry in PheOH. (bottom) View of the coiled-coil motif in PheOH (left) and TyrOH (right).

2.4. Tetramerization and the Tetramer–Dimer Equilibrium

The crystal structure of a truncated form of $hPheOH_{Cterm}$, including both the catalytic and the tetramerization domains (residues 116−452), has recently been determined.[11] This fragment of hPheOH ($hPheOH_{Cterm}$) retains full catalytic activity and is more soluble than the wild-type enzyme.[17] The $hPheOH_{Cterm}$ catalytic domain is identical within coordinate error to the structure of a dimeric $hPheOH_{Cat}$ form[12] discussed in section 2.2. The $hPheOH_{Cterm}$ catalytic domain in the tetrameric structure can be superimposed on the corresponding domain of the $rTyrOH_{Cterm}$ structure[10] with a rmsd of 0.64 Å for all the Cα atoms. The assembly of hPheOH and rTyrOH (see section 3.6) might be described by a domain swapping mechanism in which secondary structural elements mutually switch their position to promote oligomerization.[10,11] The tetramerization domain is formed by a C-terminal "arm" consisting of two β-strands, forming a β-ribbon, and a 40 Å long α-helix. The C-terminal arm extends over a neighboring monomer, bringing the four helices (one from each monomer) into a tightly packed antiparallel coiled-coil motif in the center of the structure (Figure 7). In the hPheOH structure, the tetramer is formed by two conformationally different dimers, resulting in a distortion of the 222 symmetry (in contrast to that observed in TyrOH). A superposition of the two monomers shows that the catalytic

domains and tetramerization domains, if taken separately, are identical, but they adopt different relative orientations (Figure 7). The distortion of the tetramer symmetry is also evident from a surface calculation: in $PheOH_{Cterm}$ the subunits interact with a buried surface area of about 1200 and 1700 Å^2, across the crystallographic 2-fold dimerization interfaces AC and BD, respectively. The buried surface calculated for the $TyrOH_{Cterm}$ structure is about 1600 Å^2 for both dimerization interfaces AC and BD. The discrepancy results from a change in backbone conformation at the hinge region that connects the β-ribbon to the coiled-coil helix accompanied by another rotation in the coiled-coil helix.

Two rotation points are observed in the tetramerization domain.[11] The first hinge axis is found at Thr 427, leading to a 22° movement of the catalytic domain with respect to the tetramerization domain. All the residues in the hinge region (425−429) are nicely defined in electron density, except for Thr427 which is disordered, suggestive of flexibility in this part of the polypeptide chain. The second change in backbone conformation is found at Gly 442. This residue generates a kink in the coiled-coil helix and a rotation of about 20° (Figure 7). A conformational change in the helix could be necessary to preserve the coiled-coil interactions in response to the change in the relative orientation of the subunits. In the rTyrOH sequence, Thr427 and Gly442 are replaced by a proline and histidine residue, respectively (Figures 1). It has recently been proposed that the presence of a proline in the exchanging arm induces conformational constraints on the peptide backbone that favor the optimal conformation for oligomerization.[11] Both PheOH and TyrOH sequences contain a total of three proline residues in the tetramerization domain. In $hPheOH_{Cterm}$, two prolines (Pro407 and Pro409) define the sharp turn that links the tetramerization domain to the catalytic domain. Another proline is also found at the C-terminal end of β-strand Tβ1 (residue 416), but no proline residue is located at the last hinge region connecting to the coiled coil, where the conformational change is detected. The lack of a proline residue at this position may allow more flexibility at this linker region and modulate the arrangement of the quaternary structure in hPheOH. In $rTyrOH_{Cterm}$, a proline residue is present in each of the hinge regions of the tetramerization domain, probably stabilizing its domain-swapped conformation.[11]

Full-length PheOH has been described to exist as both a tetramer and dimer[36−38] in a pH-dependent equilibrium.[39] Lowering the pH[39] as well as binding of L-Phe[36−38] shifts the equilibrium toward the tetrameric form of PheOH. By contrast, TyrOH and TrpOH are always reported to be a tetramer in solution. Truncated forms of PheOH and TyrOH in which the C-terminal domain is left intact have always been isolated as tetramers.[17,40] Removal of the last 24 residues at the C-terminus results in dimeric (PheOH) or dimeric/monomeric (TyrOH) active hydroxylases.[17,40] The architecture of the $hPheOH_{Cterm}$ tetramer[11] matches the overall fold and organization found in the structure of tetrameric $rTyrOH_{Cterm}$.[10] Despite the high degree of sequence and structural identity, superposition of $rTyrOH_{Cterm}$ and $hPheOH_{Cterm}$ shows that the relative orientation of the subunits forming the tetramer is different in the two enzymes.[11] The difference is caused by a distortion of the approximate 222-fold symmetry in the hPheOH tetramer, whereas in the rTyrOH tetramer the four subunits are related by true 222-fold crystallographic symmetry and form a dimer of dimers with only two unique subunit−subunit interfaces. With the evidence of a conformational difference between the two enzymes at hand it is tempting to hypothesize whether it is physiologically meaningful. PheOH and TyrOH share a common catalytic mechanism in which the reduced pterin cofactor, dioxygen, and iron are required to hydroxylate their respective aromatic amino acid substrates (Figure 2), but they are regulated through different mechanisms.[1] During the past few years, the mechanism of activation of PheOH by its substrate (L-Phe) has been the subject of intense biochemical and spectroscopic studies which have revealed that this activation is highly cooperative (see also section 2.5). L-Phe binds with positive cooperativity[16] and is always accompanied by alterations in the tertiary structure of the enzyme,[41−44] but the number of binding sites and the nature of the more specific conformational change(s) have not yet been ascertained.[1] Substrate activation has been proposed to involve cooperativity among all four subunits of the tetramer,[17] and radiation target analysis has shown that activation of PheOH results in modification of the monomer structure and promotes stronger association at the dimer interface.[45] These results are further supported by evidence of an increase in volume of the tetrameric rPheOH[1] and by a shift of the dimer ↔ tetramer equilibrium toward the tetrameric form upon binding of L-Phe.[36−38] Recent FT-infrared spectroscopic studies led to the same conclusion and have also shown that the alterations measured upon substrate activation of hPheOH are not accompanied by any measurable changes in the secondary structure.[44] The asymmetric structure of the $hPheOH_{Cterm}$ tetramer may represent an intermediate state and suggest that high flexibility in the tetramerization domain is required to optimally orient the domains for catalysis. Further studies are required to understand if and how the observed asymmetry of the tetramer is related to cooperative substrate activation.

A possible contribution to the conformational heterogeneity in the crystal structure of $PheOH_{Cterm}$ could be a chemical modification. $PheOH_{Cterm}$ crystals lose their diffraction intensity after a few days, and mass spectroscopy analysis shows a time-dependent heterogeneity of the protein in solution.[11] 2D-electrophoresis of full-length recombinant wild-type human PheOH (as isolated from *E. coli*) has shown a microheterogeneity in terms of the isoelectric point (five components), which has been proposed[46] and recently proven to be a result of progressive deamidation of rather labile amide groups in the newly synthesized protein. Although the sequence positions of the labile amide groups in PheOH are not yet identified, the residues have been located to the

C-terminal domain and are most probably labile Asn residues (Solstad, T.; Flatmark, T., unpublished data). The domain contains eight Asn residues (in position 133, 167, 207, 223, 376, 393, 401, and 426) which are positioned on the surface of the enzyme. Mutation of these residues may confirm if a nonenzymatic deamidation mechanism is responsible for the difficulties encountered in the crystallization of this enzyme in its tetrameric form.[11] The deamidation results in a localized increase in the negative surface charge of the catalytic domain. This effect may contribute to an increase in the solubility of the recombinant protein when expressed as fusion protein in *E. coli* and an activation of the enzyme as well as an increased susceptibility to limited tryptic proteolysis (Solstad, T.; Flatmark, T. unpublished data).

2.5. Interactions between the Catalytic and Regulatory Domains and Regulation of Enzyme Activity by Substrates and Phosphorylation

The model structure of the rPheOH regulatory *plus* hPheOH catalytic and tetramerization monomer and tetramer is shown in Figure 3. The catalytic domain of rPheOH (residues 116−424) can be superimposed onto the corresponding region in hPheOH with an overall rms deviation of 0.66 Å (all non-hydrogen atoms) and with rTyrOH catalytic domain with an overall rms deviation of 0.77 Å (all non-hydrogen atoms). The N-terminus of the regulatory domain starts off in close proximity to the opening of the active site with electron density starting at residue 16 (the first 15 amino acids are disordered in the present structure). The regulatory domain then departs away from the active site opening and is composed of the common $\beta\alpha\beta\beta\alpha\beta$ structural motif. The continued polypeptide chain then runs parallel to the N-terminus of the regulatory domain returning to the catalytic domain active-site opening. The interface between the regulatory and catalytic domains in a monomer is defined by 270 contacts, with seven principal hydrogen bonds and 10 salt bridges between the two domains and a contact surface area of approximately 1400 Å^2. In addition, there is substantial contact between the catalytic domain on one monomer and the regulatory domain of the second monomer forming a dimer. This contact surface of 600 Å^2 is defined by 104 contacts, with seven hydrogen bonds and one salt bridge.

As determined by the DALI algorithm, the catalytic domain of the aromatic amino acid hydroxylases does not share a homology with any other known protein structures. The PheOH regulatory domain, in contrast, contains a structural motif that has been seen in 60 other proteins (DALI Z-score ≥ 2). In some cases, the homology is with a known regulatory domain of a multidomain enzyme, e.g. the serine binding regulatory domain of *E. coli* phosphoglycerate dehydrogenase[47] and the nucleotide binding domain of aspartate transcarbamoylase.[48] Both of these regulatory domains contain the same $\beta\alpha\beta\beta\alpha\beta$ fold, including the same spatial ordering of the β-strands as shown in Figure 8. An important structural difference from PheOH, is that these regulatory

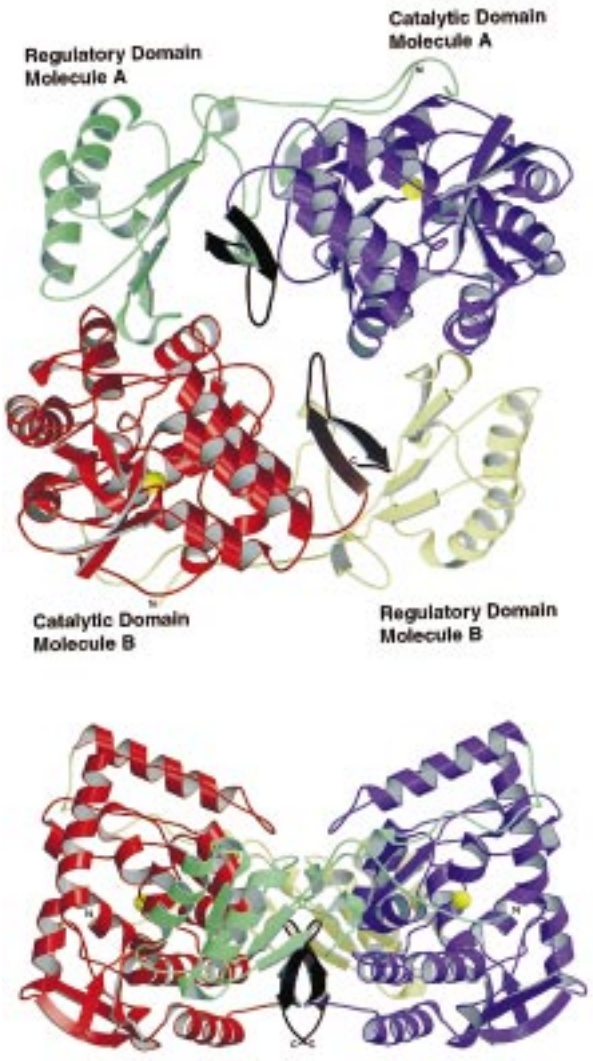

Figure 8. (top) Top-view structure of the rPheOH regulatory/catalytic domain dimer crystal structure. (bottom) Side view of same structure shown above.

domains form homodimers where the four β-strands of each monomer contribute to one continuous 8 stranded β-sheet.

In its full-length tetrameric form, PheOH is subject to allosteric regulation and activation by several chemical agents, among which the substrate (L-Phe) is of particular physiological significance.[16] A positive cooperativity is manifested both in its rate concentration curve and its equilibrium binding. In steady-state kinetics, PheOH exhibits a nonhyperbolic (sigmoidal) dependence of activity on substrate concentration (positive cooperativity), which reflects a slow transition (time scale, minutes) of the enzyme from a low-affinity to a high-affinity state,[49] characteristic of a hysteretic enzyme.[50] The underlying mechanism which accounts for these properties is, however, poorly understood, and alternative models have been proposed to explain the experimental data.[1,16,27,37,49,51] Thus, the literature contains conflicting reports about the number of L-Phe binding sites as well as the location of the binding site responsible for the cooperativity of its binding.[1] In one model the enzyme is considered to have two different binding sites for L-Phe, a catalytic site and a regulatory (allosteric)

site,[37,51] the latter being responsible for the cooperativity. Although no crystal structure information is yet available for the binary PheOH−L-Phe complex, putative binding sites for the substrate have been searched for in the nonliganded enzyme with reference to the proposed allosteric regulatory site.[16,37,51]

One possible function of the regulatory domain in PheOH may be to provide a binding site for L-Phe, i.e., an allosteric regulatory site distinct from the active site. When the regulatory domain is removed, hPheOH is no longer activated by preincubation with the substrate,[17] but this finding is no proof of a regulatory binding site outside the active site. In this discussion, activation by nonphysiological chemical agents has been considered as possible indirect supporting evidence for a second binding site.[13] Special focus has been on the alkylation of Cys237 by *N*-ethylmaleimide, which activates the enzyme to a similar extent as L-Phe preincubation and abolish the cooperative binding of L-Phe.[16] Cys237 is conserved in all known nonbacterial PheOH sequences but is replaced by an arginine in nearly all of the TyrOH and TrpOH enzymes. In the crystal structure of hPheOH, Cys237 is found on the surface of an α-helix in the catalytic domain. Its side chain protrudes into a hydrophobic pocket at the dimer interface between the catalytic domain of one monomer and the regulatory domain of the adjacent monomer. The closest contact to the sulfur atom is Pro69, 3.4 Å away. Completing the hydrophobic pocket is Phe233, which comes within 3.7 Å of the Cys237 sulfur atom. This region of the PheOH regulatory domain is spatially the same as the part of phosphoglycerate dehydrogenase[47] which makes most of the contacts to its bound serine. Pro69 in PheOH is located at the C-terminus of β-strand 2, at one corner of the rectangular-shaped regulatory domain. Likewise, most of the phosphoglycerate dehydrogenase serine contacts come from the loop between β_1 and α_1, which is at the same corner of the fold.[47]

Mitnaul and Shiman[52] proposed a heretofore unobserved in vitro and in vivo regulation scheme for rPheOH. Their model suggests that not only is L-Phe an allosteric activator of the enzyme, but also that the pterin cofactor BH_4 is an allosteric inhibitor of the enzyme. Their data have been interpreted in terms of an allosteric binding of BH_4 which results in an inactive complex which blocks L-Phe activation and also plays an important in vivo role of sequestering BH_4. The primary cellular variable in this model is still the L-Phe concentration, but now the enzyme is actively down-regulated by BH_4 when L-Phe levels are low. The data have been interpreted to support the existence of both a pterin catalytic site and a pterin regulatory site.

In light of the proposed allosteric regulatory role of tetrahydropterin, it is interesting that a known pterin binding protein is structurally homologous to the PheOH regulatory domain. The fold of DCoH/PCD contains a $\beta\alpha\beta\beta\alpha$ motif which can be superimposed on PheOH with an rmsd of 2.9 Å, although the sequence identity is just 10%. DCoH/PCD is a human protein which functions both as a dimerization cofactor of hepatocyte nuclear factor 1 (HNF-1) and as a pterin 4a-carbinolamine dehydratase. The latter function contributes to the regeneration cycle of reduced tetrahydropterin cosubstrate for PheOH (Figure 2). The crystal structure has been determined for DCoH/PCD with dihydropterin (BH_2) bound.[53] The crystal structure and site-directed mutagenesis of DCoH/PCD point to a number of residues as playing key roles. Of these, Asp61 and His63 are conserved in a sequence alignment between DCoH/PCD and PheOH. There is a higher degree of conservation when the comparison is made with the TyrOH regulatory domain where the sequence from five different species shows the His62−His63 pair from DCoH/PCD and also Glu58 which serves to activate His63. In the PheOH structure (without bound pterin), the arrangement of these residues could not accommodate a similar mode of binding. Thus, although this fold has been shown to bind pterin, the location of the putative allosteric pterin site in PheOH[52] has not yet been structurally confirmed.

In addition to the modulation of PheOH catalytic activity by L-Phe and pterin cofactor, phosphorylation of Ser16 in the regulatory domain by PKA and CaM kinase II is known to stimulate the activity of the rat enzyme.[16,42,54] Only four other enzymes have been studied structurally in both the phosphorylated and the dephosphorylated states. In the case of isocitrate dehydrogenase, phosphorylation of an active-site serine leads to inhibition through the repulsion of a carboxyl group from the substrate citrate.[55] In cyclin-dependent kinase 2 (CDK2), phosphorylation activates the enzyme 300-fold by inducing a 7 Å movement of a loop to create a competent substrate binding site.[56] Glycogen phosphorylase is activated by phosphorylation of a threonine (yeast) or serine (rabbit) residue near the N-terminus, leading to a 1300-fold activation of the yeast enzyme.[57] Thr30 in the yeast enzyme moves by 36 Å and switches from making intradimer contacts to being buried in the allosteric binding site of its own subunit, displacing the phosphate group of the inhibitor glucose-6-phosphate. The rabbit enzyme shows a ~40 Å shift in Ser14 with a switch from intrasubunit contacts to neutralization of the phosphate group in the dimer interface and subsequent ordering of the AMP allosteric activator site.

PheOH is similar to the glycogen phosphorylase in that the phosphorylation site is in a loop region near the N-terminus of the protein. PheOH, however, is very different from the enzymes discussed above in the magnitude of the kinetic effect of phosphorylation. In the absence of L-Phe preactivation of the rat enzyme, there is a 4- to 6-fold increase in specific activity upon phosphorylation of rPheOH.[42,58] For L-Phe-activated hPheOH, there is only a 1.6-fold increase in the specific activity upon phosphorylation by PKA.[59]

The rate or phosphorylation of rPheOH by PKA is under substrate-directed regulation.[42] The conformational change induced in rPheOH by L-Phe binding makes the enzyme more prone to PKA phosphorylation, which in turn sensitizes the enzyme toward activation by L-Phe.[42] Thus, phosphorylation de-

creases the $[S]_{0.5}$ for L-Phe from 51 to 26 μM. The joint operation of these mechanisms in vivo would increase the efficiency with which L-Phe controls the activity of the enzyme.[42] By contrast, the natural pterin cofactor (BH_4) is a negative effector of the phosphorylation by PKA, indicating that pterin binding also induces a conformational change in the enzyme.[42] A kinetic analysis has indicated that the effects of L-Phe and BH_4 in rPheOH are mediated by distinct sites coupled by a free energy of 3.2 kJ mol^{-1}.[42] Overall, phosphorylation appears to modify the equilibrium in favor of L-Phe activation over pterin inhibition, which is essential in order to maintain homeostatic regulation of the plasma L-Phe level.

Interestingly, the phosphorylated form of a C-terminal truncated form of rPheOH diffracted to much higher resolution, 2.2 versus 2.8 Å for the dephosphorylated form.[60] Similarly, the full-length protein yielded crystals large enough for X-ray diffraction only when it was phosphorylated. Both of these observations suggest a higher degree of order in the phosphorylated form which has recently been directly shown by FT-infrared spectroscopy of hPheOH.[44]

As predicted from the primary structure, the Ser16 phosphorylation site is part of a loosely structured region which rests on the surface of the catalytic domain (Figure 8). One turn in this N-terminal section is directly over the active site. The closest proximity for the regulatory domain to the active site iron is Ser23 with a Cβ to iron distance of 8.7 Å. The protein backbone is in a fairly extended conformation from Ser23 to the start of Rβ_1 at Ile35, which is 26 Å away. The environment of Ser16 does not provide any obvious clues about the structural role of phosphorylation. There is not a cluster of arginine residues nearby which would neutralize the phosphate charge. Positively charged residues are close by in the sequence at Arg13 and Lys14, but these are not seen in the electron density. Interestingly, phosphorylation protects Arg13 from proteolytic cleavage by Factor Xa when PheOH is expressed as a fusion protein with maltose binding protein.[59]

3. Tyrosine Hydroxylase

Tyrosine hydroxylase (TyrOH, tyrosine 3-monooxygenase, EC 1.14.16.2) catalyzes the conversion of tyrosine to L-DOPA (Figure 2), the rate-limiting step in the biosynthesis of the catecholamines dopamine, adrenaline, and noradrenaline. This reaction has been studied by steady-state kinetics,[1,9,31,32] partitioning effects of substrate substitution,[31,32] and kinetic isotope effects.[73] Somewhat contradictory conclusions have been obtained with respect to the reaction mechanism, which may partly be explained by difficulties in obtaining homogeneous preparations of the enzyme from mammalian tissues.[1,33,34] Recent steady-state kinetic studies, using recombinant rTyrOH, are consistent with an ordered reaction mechanism in which the order of binding is the pterin cofactor (BH_4), dioxygen, and L-Tyr and with the formation of a dead-end enzyme−tyrosine complex.[31,32] The rate-limiting step appears to be the slow formation of a hydroxylating intermediate which can either react rapidly with the amino acid substrate or break down nonproductively (uncoupled reaction).[73]

3.1. Catalytic Domain and Active Site

The region from residues 188 to 456 of rTyrOH has been defined as the catalytic domain ($rTyrOH_{Cterm}$).[10] Any truncation within these residues results in a protein which is more poorly expressed and has no detectable activity.[9] The $rTyrOH_{Cterm}$ contains the same secondary structure and the same arrangement as $hPheOH_{Cterm}$. This region is 49% α-helical with the remainder made up of short β-strands (9%) and long loops. In the portion of the catalytic domain closest to the tetramerization domain, the α-helices Cα8, Cα9, and Cα12 form a closely packed bundle. The rest of the helices, including the ones involved in iron binding, do not pack against other α-helices. Instead, the helices interact with loops or with small portions of α-helices. This relatively loose helical packing might contribute to the enzyme family's high susceptibility to disruption by point mutations (see section 4) and may facilitate gross conformational changes required for enzyme function. As observed for PheOH, a structural homology search of the Protein Data Bank using the DALI algorithm identified no known occurrences of protein structures similar to either the C-terminal region of TyrOH or the smaller catalytic domain.

The active site consists of a 17 Å deep cleft at the center of the catalytic domain basket. The cleft is lined primarily by four α-helices: α6, α7, α8, and α9. The opening into the active site is guarded by two loops (residues 423−428 and 290−296) that come to within 12 Å of each other as they reach over the top of the 30 Å wide active site. The active site is 15 Å across in the perpendicular direction. The N-terminus of the C-terminal region is located near this open face in a reasonable position for placement of the regulatory region, which has been postulated to function by directly controlling the accessibility of substrate or cofactor to the active site.[61]

The iron atom is 10 Å below the enzyme surface within the active site cleft. The iron is directly coordinated by His 331 (N···Fe 2.1 Å), His 336 (N···Fe 2.1 Å), and Glu 376 (O···Fe 2.1 Å) (Figure 5). Both His 331 and His 336 have been previously shown by site-directed mutagenesis to be required for iron binding. All three iron-coordinating residues are completely conserved in the known aromatic amino acid hydroxylases. Also conserved is Gly335, which accommodates a distinct bend in α-helix Cα7. This bend decreases the distance between His331 and His336, allowing these side chains to coordinate the iron. The iron environment of two neutral histidines and an anionic carboxylate is in agreement with Mössbauer and X-ray absorption (XAS) spectroscopy of hTyrOH.[21] Electron density is also observed for two water molecules at a distance of 2.0 Å from the iron. The coordination geometry is square pyramidal with His331 as the axial ligand and two water molecules joining the protein ligands in the equatorial positions. The iron atom is observed to be in the plane of the equatorial ligands. The region opposite axial ligand

His331 is distinctly void of density where a possible sixth ligand, as observed by Mössbauer and XAS spectroscopy of the catalytically active Fe(II) form,[21] would be located. However, a highly mobile water molecule located there cannot be ruled out. The aerobic conditions at which the iron-cocrystals were grown suggest that the iron in this structure is in the oxidized Fe(III) state. The overall iron coordination is very similar to that seen recently in the crystal structures of both the ferric and ferrous forms of an iron-utilizing bacterial extradiol dioxygenase and is referred to as a 2-His-1-carboxylate facial triad.[29]

Immediately surrounding the iron binding site are a number of highly conserved residues that may play important roles in catalysis. For instance, phenylalanine residues at positions 300 and 309 are completely conserved in the 16 known mammalian gene sequences in this family. In the crystal structure of rTyrOH, these residues are exposed on the surface of the active site and point toward the iron with Phe C^{ξ} to Fe distances of 6.0 and 5.3 Å, respectively. These phenylalanines may help to attract the hydrophobic portions of the substrate and cofactor (see section 3.2).

Pro327 is also conserved in all known sequences in the family. The mutation Pro327Leu has been shown to reduce the enzyme activity due to a 20-fold increase in K_m for the tetrahydropterin cofactor.[62] On the other hand, mutating this residue to alanine does not substantially affect the K_m value for the cofactor, but it does eliminate strong substrate inhibition of the enzyme. These data are consistent with enzyme kinetic studies in which L-Tyr is shown to be a competitive inhibitor versus tetrahydropterin at concentrations above 150 μM.[31,32] In the structure, Pro327 noticeably protrudes into the active site. The proline's C^{β} and C^{γ} are 4.8 and 5 Å, respectively, from the active site iron atom.

3.2. Binding of the Pterin Cofactor and Analogues at The Active Site

The residues near the iron in rTyrOH are well conserved in the aromatic amino acid hydroxylase family. The three hydrophobic residues Phe300, Phe309, and Pro327 are completely conserved, and the interatomic distances between Phe300 and the π-stacked pterin are about 3.5 Å (Figure 9). Similar aromatic π-stacking arrangements are seen with a phenylalanine in the structure of chicken dihydrofolate reductase complexed with biopterin[63] and with a tryptophan in the structure of nitric oxide synthase with tetrahydrobiopterin bound.[64] In the TyrOH complex, the pterin is about 10° offset from being parallel with the benzene ring of Phe300. In dihydrofolate reductase, this offset is about 37°.[63] Several hydrogen bonds also contribute to pterin binding in TyrOH: N-8 of the pterin ring forms a hydrogen bond with the main-chain carbonyl of Leu295. The adjacent glycine at position 293 is conserved in all 14 known eukaryotic aromatic amino acid hydroxylases and most likely allows for flexibility in this loop region, which is important for pterin binding (Figure 9 (bottom)). The carbonyl at position C-4 of the pterin ring forms a 3.2 Å hydrogen bond with the highly conserved residue Tyr371. Two additional hydrogen bonds are formed by the dihydroxypropyl group attached to C-6. The hydroxyl at position C-1′ forms a hydrogen bond with the main-chain amide of Leu294, and the hydroxyl at C-2′ forms a hydrogen bond with an iron-coordinating water. This hydroxyl is also 4.0 Å from the carboxyl of the conserved residue Glu332.

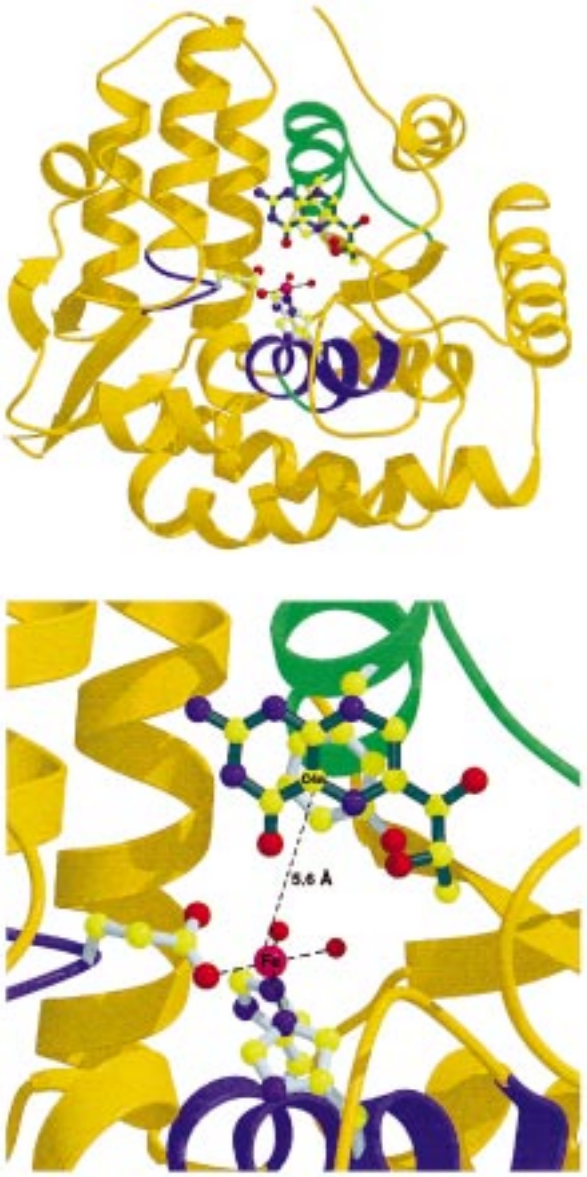

Figure 9. (top) View of the pterin-bound TyrOH structure looking directly into the active-site cleft of the catalytic domain. The three iron-coordinating residues (His331, His336, and Glu376) are shown in ball-and-stick format, as is the hydroxylated Phe300 which is behind the pterin. Coordination of the three residues and two waters to the iron is represented with dashed lines. The secondary structure portions containing the iron-coordinating residues are shown in blue, and the glycine which accommodates a kink in the His331 and His336 helix is shown in green. The helix which contains Phe300 and the adjacent loop region which participates in pterin binding is also shown in green. (bottom) A closer view of the pterin binding site. This figure was prepared with MOLSCRIPT[99] and Raster3D.[100]

The pterin-bound and ligand-free structures are isomorphous with an rmsd of 0.18 Å, well within the

experimental error.[15] No major conformational changes are observed between the two structures. Seven water molecules, which are observed in the active site of the TyrOH ligand-free structure, are displaced upon pterin binding, but the two waters which are coordinated to the iron in the ligand-free structure are unchanged in the binary complex. In both structures, the iron atom lies in the plane formed by the ligands His336, Glu376, and two water molecules (Figures 5 and 9). His331 forms the axial ligand to complete the square-pyramidal geometry (Figure 5b). In hPheOH, a third water molecule opposite the axial His285 completes an octahedral geometry. Water binding at this same position in TyrOH appears to be blocked due to a different position of Glu376/Glu330 in the two structures.[12,14] However, the ligand-free rTyrOH structure shows density for a water molecule 3.1 Å away from the iron in this axial position. That water is displaced upon pterin binding by the carbonyl oxygen attached to C-4. This oxygen, at a distance of 3.6 Å, is the closest contact between the pterin and the iron.

A wide variety of pterin analogues have been examined as substrates for the aromatic amino acid hydroxylases.[65] Substitutions of the dihydroxypropyl group are well tolerated but do affect the kinetic parameters, including the cooperativity of cofactor binding (Flatmark et al., unpublished results). Three hydrogen bonds link the dihydroxypropyl group to protein main-chain atoms or one of the water molecules coordinated to the iron. The role of these hydrogen bonds is seen in rTyrOH as a 2- to 5-fold increase in K_m value for the pterin when 6-methyltetrahydropterin is substituted for tetrahydrobiopterin BH_4.[65] Hydrophobic portions of the dihydroxypropyl binding pocket are formed by Leu294, Pro327, and Val291. The hydrophobic aspect of this pocket may explain the 10-fold decrease in K_m value for the cofactor when 6-phenyl and 6-cyclohexyl pterins are used as substrates.[25] The lack of activity observed with a 6-carboxylate[24] moiety may be due to an electrostatic repulsion by the nearby acidic residue Glu332.

The ability of 2,4,5-triamino-6-hydroxypyrimidine to function as a substrate for rPheOH[66] has suggested a minimum configuration for the pterin. Enzyme activity with the pyrimidine suggests that positions 6 and 7 of the pterin ring are not required for activity, and these positions are among the furthest from the iron in the crystal structure (6.5 and 7.6 Å, respectively). The pyrimidine retains the one hydrogen bond seen from the pterin ring system at N-8. Substitution of the carbonyl at C-4 with an amine was also seen for the active substrate 6-methyl-2,4-diaminotetrahydropterin,[24] suggesting a nonspecific role for this substituent of the pterin which is 3.6 Å from the iron in the crystal structure. Substitution of the amine at position C-2 of the pterin with an oxygen or hydrogen has been shown to eliminate PheOH enzyme activity,[24] although no direct contact of this substituent with the protein is seen in the crystal structure. A methylamine at this position is tolerated, but the dimethylamine is not.[67]

For both PheOH and TyrOH, the apparent K_m values for their amino acid substrates and dioxygen vary with the pterin cofactor used.[65] For example, the K_m value of tyrosine is 10−20 times lower when tetrahydrobiopterin is used as cosubstrate, compared to 6,7-dimethyltetrahydropterin.[65] This observation, combined with the ordered binding of pterin before oxygen and tyrosine as observed for rTyrOH[31,32] suggests that the pterin itself may form part of the binding surface for the tyrosine substrate.

Alternative biochemical approaches have previously been tried to identify the cofactor binding site in PheOH and TyrOH. A pterin analogue, 5-[(3-azido-6-nitrobenzylidene)amino]-2,6-diamino-4-pyrimidinone, has been used to probe the active site of PheOH by photoaffinity labeling but with limited success.[68] A putative pterin-binding sequence has been identified in the two hydroxylases based on the generation of a monoclonal anti-idiotype antibody which mimics the pterin molecule.[22] The antibody binds to PheOH and TyrOH, but binding is prevented when 6,7-dimethyl-7,8-dihydropterin is present. It has also been shown to bind to a diverse range of pterin-related enzymes, including dihydropteridine reductase and sepiapterin reductase, enzymes involved in the regeneration and biosynthesis of the reduced cofactor, respectively. This monoclonal antibody was found to bind to a peptide corresponding to residues 310−336 of rTyrOH, which was proposed to represent the pterin binding site.[22] In the binary complex structure (Figure 9), Gln310 and Cys311 have C_αs which are less than 5 Å from the pterin but their side chains point away from the active-site surface. Residues 312−326 form an extended loop which is completely buried in the interior of the enzyme. Pro327 forms part of the active-site surface and is within 5 Å of the iron. In the binary complex, Cγ of Pro327 is 3.2 Å from the pterin hydroxyl at C-2′. Mutation of this residue to an alanine in TyrOH (Pro281) or PheOH results in an active enzyme which shows only a small increase in the K_m value for tetrahydrobiopterin,[62] indicating that Pro327 is not required for pterin binding. Mutation of this residue to a longer, hydrophobic leucine side chain, however, affects more the pterin binding as seen by a 20-fold increase in the K_m value for tetrahydrobiopterin in TyrOH. In PheOH, proline 281 to leucine mutation results in an unchanged K_m value for BH_4 but causes a 20-fold increase in K_m for L-Phe and a 100-fold decrease in specific activity.

The other residue in this region which has been examined by mutagenesis is Glu332. In the binary complex structure, Glu332 forms a hydrogen bond with the pterin hydroxyl at C-2′. Mutation of this residue to an alanine in rTyrOH has been reported to have little effect on enzyme activity or K_m for tetrahydrobiopterin.[62] This is not unexpected since 6-methyltetrahydropterin lacks a C-2′ hydroxyl group but is only slightly inferior to tetrahydrobiopterin as a cofactor in the rTyrOH-catalyzed reaction.[65] In contrast, mutation of the corresponding glutamic acid in PheOH (Glu286) results in a 100-fold increase in K_m value for tetrahydrobiopterin.[69] Thus, the role of the glutamic acid in binding the dihydroxypropyl

portion of the pterin may be more important in PheOH than in TyrOH.

3.3. Spectroscopic Studies on the Binding and Conformation of the Cofactor

Mössbauer and XAS spectroscopy studies of hTyrOH have shown that there are no major changes in the first coordination shell of the iron upon addition of tetrahydrobiopterin.[21] However, the iron center of both TyrOH and PheOH is known to be reduced to the active Fe(II) state by a reaction involving an oxidation of the reduced pterins.[1] Catechols, which have been shown by resonance Raman spectroscopy to directly coordinate the Fe(III) in bTyrOH,[33] are competitive inhibitors versus the pterin cofactor but noncompetitive inhibitors versus the tyrosine substrate.[26] Crystallographic studies of catechols bound to hPheOH have shown that the catechol binding site spatially overlaps with the pterin binding site.[14] Taken together, these results suggest that the pterin binds in close proximity to the iron but is not coordinated to it. The crystal structure is in accordance with these results, with the carbonyl oxygen attached to C-4 making the closest contact to the iron at a distance of 3.6 Å.

Proton NMR has been used to study the conformation of 7,8-dihydrobiopterin, 6-methyltetrahydropterin, and 3-methyltetrahydropterin bound to the active site of hTyrOH.[23] In these studies, the active-site iron was replaced with cobalt and metal−proton distances were measured by the paramagnetic probe-T_1 method. From the measured distances, families of models were calculated to estimate the distance from the metal to pterin C-4a position which is hydroxylated during enzyme turnover. The NMR measurements are generally in agreement with the crystal structure analysis,[15] especially with regard to the metal being closest to the O-4, C-4a, and N-5 portion of the pterin. There is also agreement about the dihydroxypropyl group of the pterin being in a closely packed almost cis conformation as compared to the extended trans conformation of the free pterin, such that the C-3′ methyl group is relatively close to the metal. The NMR models of bound 7,8-dihydrobiopterin show the conformation of the hydroxyls at C-1′ and C-2′ to have a dihedral angle of $\Theta = 75-83°$, whereas the crystal structure has a dihedral angle at this position of $\Theta = 120°$. From the crystal structure, one would expect the methyl group of 3-methyltetrahydropterin to be in steric conflict with Tyr371 and Glu376 of the enzyme, explaining the low affinity of this analogue in steady-state kinetics[23] and equilibrium binding (Flatmark et al., unpublished data). This conflict could explain the generally longer metal−pterin distances seen in the NMR measurements with 3-methyltetrahydropterin. Overall, as seen by Mössbauer and XAS spectroscopy, the NMR data have revealed that the pterin is close to the metal but not coordinated to it.

3.4. Meta Hydroxylation of Phe300

Examination of the pterin-bound and reexamination of the pterin-free tyrosine hydroxylase structures revealed a peak of electron density at a distance of 1.4 Å from one of the *meta* carbons in the benzene ring of Phe300.[15] This density appears to represent hydroxylation of Phe300 in the *meta* position and subsequent hydrogen bonding to the main-chain carbonyl of Gln310. Mass spectrometry analysis of the purified TyrOH shows a molecular mass which was 11−16 mass units too high for the known sequence, which is in accordance with the hydroxylation of this phenylalanine. No other protein modifications were observed in the *E. coli* expressed protein. The hydroxylated carbon of Phe300 is 3.9 Å from the C-4a carbon of the pterin, which is hydroxylated during enzyme turnover, and 6.6 Å away on a direct, unobstructed path from the iron. Both of these distances are very similar (4.0 and 6.9 Å) when taken from the other *meta* carbon of Phe300. Interestingly, the equivalent of rTyrOH Phe300 in hPheOH (Phe254) does not appear to be hydroxylated and in fact does not have especially good density compared to other active-site residues.[11,12,14] The hydrogen bond which is formed as a result of the meta hydroxylation of Phe300 may serve to stabilize the position of this residue and allow for easier pterin binding to the active site.

Both rTyrOH and hPheOH used for the published structural studies[10−15] were expressed in *E. coli* strain BL21/DE3. This bacteria is known to contain pterin substrates for these enzymes[70] and dihydropteridine reductase for regenerating tetrahydropterin.[71] PheOH has been shown to strongly discriminate against the hydroxylation of tyrosine at the *meta* position,[61] thus preventing in vivo the unwanted diversion of its reaction product. The presence of the *meta* hydroxylation of residue Phe300 only in TyrOH may be related to this difference in substrate specificity between the two enzymes.[61,72]

3.5. Hydroxylation Reaction and Regulatory Properties

As seen from Figure 2, PheOH and TyrOH catalyze very similar reactions and thus generate very similar oxygenating intermediates.[1] Recently, the reaction of dioxygen in rTyrOH has been examined by ^{18}O kinetic isotope effects.[73] These studies have revealed a change in bond order of the dioxygen in the rate-determining step, and a magnitude of the isotope effect indicating that the formation of an iron−dioxygen species is not rate-determining. This result, in combination with previous studies, led the authors to suggest that a one-electron transfer from the tetrahydrobiopterin to dioxygen forms a superoxide anion as the first reactive intermediate. This radical pair would then couple to form a 4a-peroxytetrahydrobiopterin intermediate which may or may not interact with the iron.

The position of the pterin relative to the active-site iron, as observed in the binary crystal structure (Figure 9),[15] easily accommodates the 4a-peroxytetrahydrobiopterin intermediate, with possible bridging to the iron, which has previously been proposed by several groups.[74−76] Pterin binding is seen to displace a water 3.1 Å from the iron in rTyrOH and could possibly displace one of the coordinated waters of

hPheOH. The resulting binary complex has a distance from the iron to the hydroxylated pterin C-4a carbon of 5.5 Å. Therefore, dioxygen could simultaneously interact with the ferrous iron and the C-4a position. The region in the structure between the iron and the C-4a carbon is buttressed by the completely conserved residues Phe309 and Pro327. The hydrophobic region formed by one of these two residues may promote dioxygen binding. Kinetic experiments show rapid equilibrium binding of dioxygen, indicating weak binding of dioxygen to the binary complex.[31] The axial water which coordinates to the iron and is 5.1 Å from C-4a of the pterin might be displaced during the hydroxylation reaction.

The proximity of the pterin to the iron in TyrOH can provide insight regarding the iron requirement of pterin-dependent monooxygenases compared to the metal-free catalysis of flavin-dependent monooxygenases.[77] Tetrahydrobiopterin free in solution has a pseudo-first-order autoxidation rate constant of $\sim 10^{-6}$ s^{-1}, compared to productive turnover numbers of ~ 6 s^{-1} for PheOH and ~ 2 s^{-1} for TyrOH.[61] In contrast, the reaction of flavins with dioxygen is several orders of magnitude faster than pterin oxidation; the reaction rates of flavoproteins range both above and below the autoxidation rate.[78] Another difference with the flavoproteins, and possible role for the iron, is the ability of the aromatic amino acid hydroxylases to react with unactivated aromatic and aliphatic C−H substrates. Further studies of other pterin- and iron-dependent monooxygenases as eukaryotic glyceryl−ether monooxygenase (EC 1.14.16.5), bacterial anthranilate 3-monooxygenase (EC 1.14.16.3), and mandelate 4-monooxygenase (EC 1.14.16.6) should contribute to a better understanding of the pterin−iron interaction in the aromatic amino acid hydroxylases.

In its full-length tetrameric form TyrOH is subject to several posttranslational mechanisms of regulation including phosphorylation (in the regulatory domain),[65] end-product (catecholamine) inhibition,[26,33,35] and substrate (L-Tyr) inhibition.[65] In addition, it has recently been demonstrated that the natural cofactor (BH_4) also has an important regulatory function.[78b] The cofactor binds to tetrameric hTyrOH (isoform 1) with a pronounced negative cooperativity ($0.4 < h < 0.6$) as determined by kinetic analyses and equilibrium binding.[78b] Interestingly, phosphorylation of Ser40 (regulatory domain) by protein kinase A amplified the negative cooperativity ($h = 0.3$) and decreased the concentration for half-maximal activity from 24 to 10 μM.[78b] Thus, in contrast to the structurally and functionally homologous catabolic enzyme PheOH which demonstrates a positive cooperativity of L-Phe binding/activiation (section 2.5), the negative cooperativity of BH_4 binding to hTyrOH creates an efficient way to regulate catecholamine biosynthesis in response to changes in the cofactor concentration within a narrow and low micromolar range, corresponding to the concentrations estimated in catecholaminergic neuroendocrine cells.[78b]

3.6. Tetramerization of Tyrosine Hydroxylase

$TyrOH_{Cterm}$ forms a tetramer with two distinct oligomerization interfaces.[10] Two monomers (Figure 7) interact across a dimerization interface (1654 Å^2 buried surface area) which involves both the catalytic domain and the tetramerization domain. The dimerization interface between just the catalytic domains of the first two monomers consists mostly of hydrogen bonding interactions and a salt bridge (Lys170 to Glu282). The second monomer interface on the other hand, interacts solely through the tetramerization domain (539 Å^2 buried surface area).

Expression of truncated forms of the catalytic region of hPheOH and rTyrOH have shown that removal of the tetramerization domain yields enzymatically active protein in a dimeric form (hPheOH)[17] and a dimeric/monomeric form (rTyrOH).[79,80] The tetramerization domain of TyrOH consists mainly of the 24 residue Tα1 (Figure 1) which contains a hydrophobic heptad repeat that is conserved within this family of hydroxylases.[10,11] The Tα1 helix forms an antiparallel coiled coil with 222 crystallographic symmetry which spans the full 40 Å width of the tetramer but does not extend into the solvent (Figure 7). The coiled coil, which has a slight left-handed superhelical twist, creates a cylinder in the middle of the four monomers with dimensions of ~ 10 by ~ 15 Å. The helices interact with each other mainly through the contacts of the small hydrophobic residues of the heptad repeat (Figure 7). While proline residues are not usually observed in heptad repeats, Pro473 from the first "a" position packs closely in the coiled-coil structure with Ile497.

Two β-strands (Tβ1 and Tβ2) and the loop that precedes them make up the rest of the tetramerization domain connecting the C-terminal helix to the catalytic domain. These structural elements may be involved in orienting helix Tα1 in such a way as to promote oligomerization (see also section 2.4). β-Strand Tβ1 interacts directly with helix Tα1 through a salt bridge between Lys459 and Glu 486.

4. Inborn Errors of Metabolism and Aromatic Amino Acid Hydroxylases

Phenylketonuria (PKU) was one of the first recognized inborn errors of metabolism,[81] and it was the first known cause of mental retardation.[82] The disease is caused by a deficient function of PheOH, inherited in an autosomal recessive fashion. Mutations in the hPheOH gene represent the most prevalent disorder of amino acid metabolism. The most severe variants result in phenylketonuria (PKU) which is characterized by high levels of L-Phe (>1000 μM) in the blood. Toxic levels of phenylalanine affect neuronal development, in particular axonal maturation, with a secondary hypomyelination which is severely inhibited during a critical developmental period.[83] The result is irreversible alterations in the architecture of the brain leading to mental retardation, if the patient does not begin treatment with a low-phenylalanine diet at an early age. Classical PKU is an autosomal recessive metabolic disorder with a frequency of approximately 1 in 10 000 Caucasians. At present, more than 300 different mutations have been identified in the hPheOH gene (see PAH Mutation Analysis Consortium database: *http://www.mcgill.ca/pahdb*).[84] Most of them are

associated with PKU, and only a small number of different mutations have been identified among non-PKU hyperphenylalaninemia (HPA) patients. The current spectrum of alleged PKU/HPA mutations consists of ~60% missense mutations, ~13% splice mutations, ~13% deletion mutations, ~6% nonsense (termination) mutations, and a few insertion mutations. Mutations have been identified in all 13 exons, but the majority are found in the 3′-half of the gene. Recombinant proteins of only 36 different PKU-related PheOH mutations have so far been analyzed in at least one in vitro expression system. These 36 sites are mapped onto the full-length PheOH structure (Figure 10 (top)).

In the structurally related hTyrOH gene only two mutations have been found, so far, to be related to neurological disorders of the basal ganglia.[4,5] Assuming that mutations are equally distributed in the genome, several alternatives can be offered to explain these differences. In contrast to the "knock-out" mutations in the hPheOH gene, complete loss of in vivo hTyrOH activity leads to death at a late stage of embryonic development or shortly after birth.[85] This may explain the large difference in the observed numbers of patients with L-DOPA responsive dystonia/juvenile parkinsonism and phenylketonuria. Another explanation may be that mutations in the hTyrOH gene are also associated with other disorders in which the metabolic/clinical phenotypes are not yet identified.

4.1. Structural Aspects of Phenylketonuria and Hyperphenylalaninemia

To date, most of the mutations have been characterized only at the DNA level.[84,85] Recent genotype−phenotype correlation studies have revealed that the hPheOH genotype does not sufficiently explain the mutant phenotype in all cases, implying that other factors are involved in the emergent property of plasma phenylalanine homeostasis.[84] However, very little information has been achieved with respect to the molecular mechanisms leading to the phenotypic heterogeneity.[85] In vitro expression of recombinant forms of hPheOH represents the only practical approach for the study of the wild-type and mutant enzymes to obtain a detailed characterization of their catalytic, regulatory, and stability properties.[85] Expression analyses in several complementary in vitro systems of mutant PheOH proteins leading to PKU/HPA have thus identified at least three groups which differ in their kinetic behavior and/or stability in vivo, i.e.: (i) mutations affecting both kinetic and stability properties of the enzyme; (ii) structurally stable mutations with altered kinetic properties; and (iii) mutations with normal kinetics but reduced stability in vitro and in vivo.[85]

The 107 mutations within the catalytic domain are rather evenly distributed throughout the structure. From a structural point of view, these mutations can be grouped into three categories : (i) mutations in the catalytic domain that are away from the active site; (ii) mutations that directly alter active-site residues; and (iii) mutations that affect the tetramerization domain.[11,12] It is interesting that no PKU/HPA mutations have been found at any of the residues involved in the coordination of the catalytic iron atom. The closest mutation is in Phe331, which is next to the iron-coordinating Glu330 (Figures 1 and 5b). Twenty-two missense point mutations have been observed in residues lining the active-site crevice, and six of these (residues 263, 265, 278, 280, and 281) are found in the putative pterin binding motif proposed by Jennings et al.[22] Many of these mutations are associated with PKU/HPA, but only five of the mutations have been expressed in vitro (Figure 10 (bottom)).[12] The Glu280Lys mutation in the putative pterin binding motif[22] is of particular interest. There are only two free charged groups in the crevice of the holoenzyme (both glutamic acids), and substitution of one of them (Glu280) by a Lys represents a dramatic change in the electrostatic potential of the crevice. However, expression of this mutant form of rPheOH in *E. coli* resulted in an enzyme with a moderately reduced specific activity (~30% of wt of rPheOH) and a slightly increased apparent K_m value for the pterin cofactor (BH_4).[69] One of the most frequent PKU/HPA mutations in southeastern Europe is Pro281Leu.[86] The substitution of Pro281 with a Leu almost certainly changes the conformation of the active site by removing the conformational constraints imposed by a proline; Pro281 is very close to the iron atom (5.3 Å). A second frequent PKU mutation is Leu255Ser in black Americans.[87,88] In this mutation a nonpolar group is substituted with a smaller polar side chain in a hydrophobic environment and is expected to result in significant structural perturbation. As expected, the substitution of Leu255 with a Ser has a more dramatic effect on the catalytic (residual) activity than substitution with a Val when expressed in three different systems in vitro.[89] Leu255 appears to be critical in controlling the separation of helix Cα6 and helix Cα9.[12] In addition to these active-site mutations, the molecular basis for the metabolic defect has recently been characterized for five missense point mutations (Arg252Gly/Gln, Ala259Val/Thr and Arg270Ser) and a termination mutation (Gly272X) in the evolutionary conserved motif of exon 7 in the catalytic domain.[89] All these PKU mutations resulted in variant hPheOH proteins which revealed a defect in oligomerization, an increased sensitivity to limited proteolysis in vitro, reduced stability in A293 cells, and a variable reduction in the catalytic activity of isolated recombinant enzymes.[89]

The splicing mutation IVS12ntg→a in intron 12 of the hPheOH gene is the most prevalent PKU allele among Caucasians.[90] The clinical and metabolic phenotype of homozygotes with the mutation is a severe ("classical") form of PKU. The mutation leads to the synthesis of a truncated form lacking the last 52 C-terminal amino acids, which include the tetramerization domain. Expression studies in eukaryotic systems indicated that the deletion abolished PheOH activity in the cell as a result of protein instability. Another frequent allele is caused by a CGG-to-TGG transition in exon 12, resulting in an amino acid substitution Arg/Trp at position 408. This mutation also results in undetectable levels of PheOH

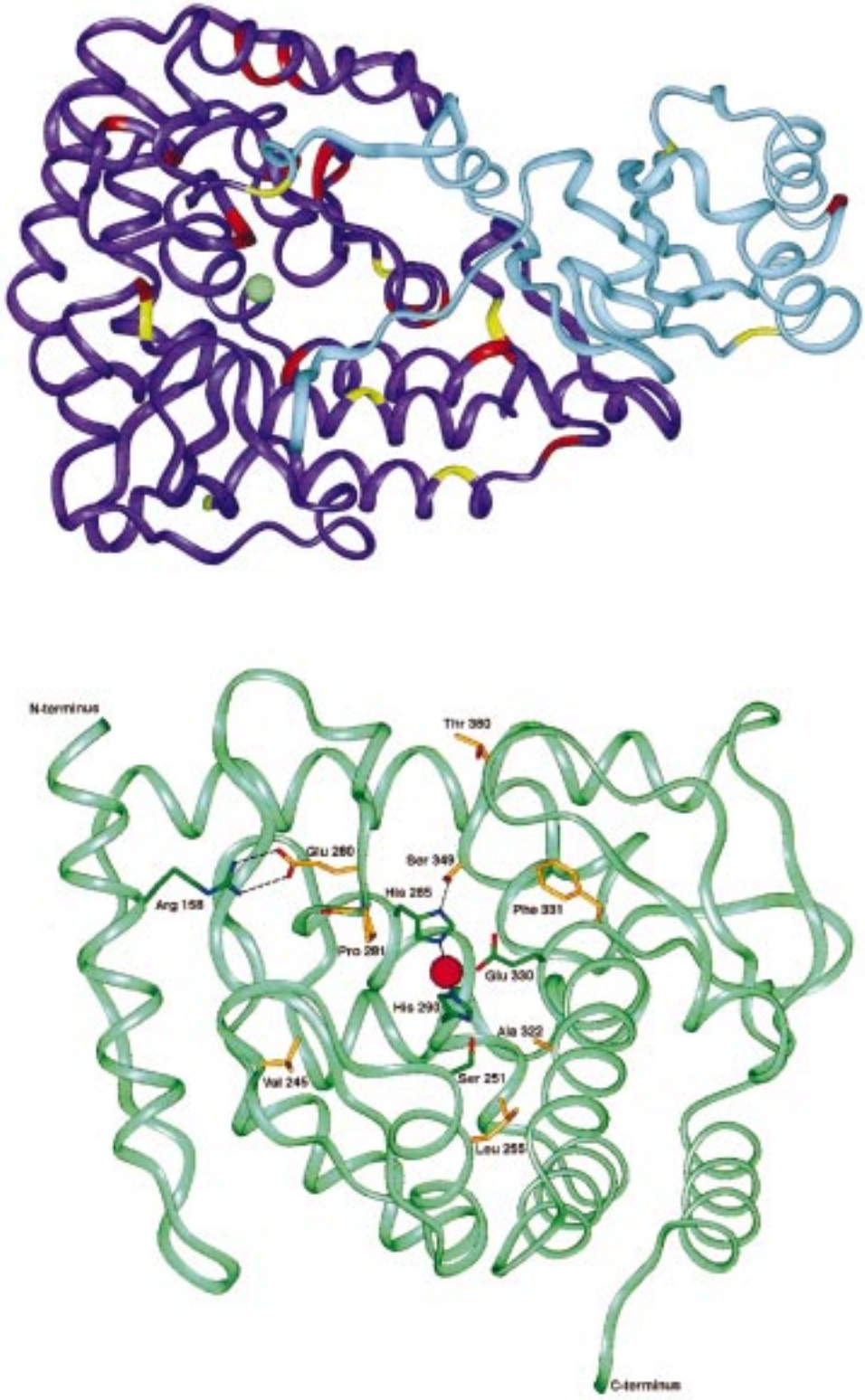

Figure 10. (top) PKU mutations mapped onto the PheOH structure in which the residual enzyme activity and/or the PheOH immuno-reactive protein has been determined in different in vitro expression systems. To date, only 36 PKU mutations have been carefully examined at 30 different residue sites. The main chain catalytic and tetramerization domains are colored blue, and the regulatory domain is colored light blue. The severe phenotypes (classical PKU) are shown in red (M1V missing from structure; G46S, R157N, R158Q, F161S, S231P, R243Q, R243X, G247V, R252W, R252G, R252Q, L255V, L255S, A259T, A259V, R270S, G272X, E280K, P281L, F299C, L311P, S349P, R408W, R413P) and the mild phenotypes (HPA) in yellow (I65T, A104D, D143G, P244L, P261Q, A322G, L348V, V388M, A403V, R408Q, Y414C). The view is down the tetramerization domain which is difficult to observe and not critical for the figure since only two mutations occur in this region and none in the coiled-coil motif. For reference, see PAH Mutation Analysis Consortium database ((http://www.mcgill.ca/pahdb) and refs 12 and 89. (bottom) View of seven residues lining the active site that cause PKU/HPA. The main-chain ribbon is colored light green. PKU/HPA mutations have the carbon atoms in yellow, and residues which interact with the mutant site residues and the iron atom are colored dark green.[12]

in vivo and in vitro and a severe metabolic PKU phenotype.[91] Analysis of the TyrOH and PheOH structures shows that the highly conserved Arg 408 is located on the hinge loop that connects the tetramerization arm to the core of the PheOH monomer, flanked by the above-mentioned Pro407 and Pro409.[11] The arginine side chain is buried and forms a hydrogen bond with the main-chain carbonyl of Leu308, Leu309, and Leu311 at the C-terminal end of helix Cα8. Arg408 could be involved in stabilizing domain swapping and promoting oligomerization by anchoring the tetramerization arm onto the catalytic domain in a proper orientation. Correct alignment of arm exchange in domain swapping is believed to be necessary for the association process (see also section 2.4). This suggestion is consistent with the analysis of the mutation R408Q that causes a non-PKU hyperphenylalaninemia in homozygotes. Expression of R408Q mutants in *E. coli* results in the synthesis of a tetrameric form of the enzyme with relatively high (~35%) residual activity of isolated recombinant enzyme (Knappskog, P. M.; Bjørgo, E.; unpublished data). The mutations Arg252Gly/Gln, Leu255Val/Ser, Ala259Val/Thr, and Arg270Ser also result in extremely reduced levels of hPheOH and are associated with severe PKU phenotypes.[89] The same is true for Phe299Cys[88] and Leu311Pro,[92] and as described above, the carbonyl atom of Leu311 forms a hydrogen bond with Arg408. The residue Ala259 is buried in a hydrophobic pocket about 4 Å from Leu311 and Leu308; a larger or polar residue cannot be accommodated without disturbing the surrounding environment. Phe299 is also involved in hydrophobic interactions that stabilize the helix where Leu311 is located, and Arg252 forms a hydrogen bond with the carbonyl atom of Ala313. These mutations map in the same region as Arg408 and dramatically alter the hydrogen-bond network or produce steric hindrance, interfering with the correct positioning of the β-ribbon (Tβ1 and Tβ2). It is likely that their effect will have consequences for the arrangement of the catalytic and tetramerization domains and thus on the normal oligomerization process. The mutation Tyr414Cys has also been reported, and the expressed enzyme retains approximately 50% of normal activity.[87] The mild effect of this mutation can be explained at the structural level: a substitution Tyr → Cys in this position should not have drastic consequences on the interactions with the neighboring residues. One of the most frequent alleles in the Oriental population is the missense mutation Arg413Pro in exon 12, which causes a severe metabolic form of PKU.[93] This mutation results in protein instability with almost undetectable levels of PheOH when expressed in eukaryotic cells.[93] Arg413 is located in the middle of the first strand (Tβ1) of the β-ribbon in the tetramerization domain (Figure 1). A proline residue in this position would disrupt the main-chain to main-chain hydrogen bond network that stabilizes the β-ribbon. The PKU mutation Arg413Pro most certainly leads to extreme disorder of the tetramerization arm, thus compromising the normal oligomeric state and stability of PheOH. The analysis of these mutations suggests that changes in the β-ribbon have major effects on the stability of the enzyme. The observation that the β-ribbon represents a mutation hot spot (http://www.mcgill.ca/pahdb) points to the structural importance of this element.

Biochemical and structural studies on hPheOH have revealed that the protein architecture is very sensitive to single-point mutations throughout the enzyme.[89] The relatively loose helical packing might contribute to the high susceptibility to disruption by point mutations. The misfolding caused by the mutations is revealed as an increased aggregation in prokaryote expression systems and as reduced stability toward intracellular proteolysis in eukaryotic expression systems and probably also in vivo.[89] The hPheOH protein has been found to be a substrate for the ubiquitin conjugating enzyme system,[46] suggesting that the proteasomes may be involved in its degradation. This mechanism of protein degradation may have particular significance with respect to the turnover of mutant forms of the enzyme.[46,85] The interesting trend observed so far on the structural vulnerability of PheOH has to be further examined as more mutations are carefully characterized by expression in complementary in vitro systems. It does suggest, however, that this family of enzymes (i.e., aromatic amino acid hydroxylases) have not been selected for stability in terms of handling single-point mutations, in contrast to many other enzymes that are necessary for cell life and capable of handling single-point mutations at many different regions in the protein structure.

4.2. Tyrosine Hydroxylase and Inherited Diseases: Structural Implications

Catecholamines (dopamine, noradrenaline, and adrenaline) are important neurotransmitters and hormones that are involved in and regulate a number of vital processes/functions in the mammalian body. During the past few years considerable progress has been made in the elucidation of the metabolic pathways involved in catecholamine biosynthesis, including kinetic and regulatory properties[1,9,94,95] as well as crystal structure analysis of the different enzymes involved in cofactor biosynthesis/regeneration and the hydroxylation reaction.[10,94,96,97] The discovery of mutations in the human enzymes have provided important clues to the pathophysiology of some inherited neurological disorders as well as to their diagnosis and treatment. Furthermore, the mutations have contributed significantly to elucidate basic regulatory properties of mammalian catecholamine metabolism.

Considering the high frequency of mutations in the hPheOH gene (see section 4.1), mutations in the hTyrOH gene have been predicted and actually found in the group of patients with L-DOPA responsive dystonia[4] and juvenile parkinsonism.[5] Furthermore, current research has suggested a link between the hTyrOH locus and bipolar affective disorders.[6] Genetic studies have also pointed to an association of hTyrOH gene polymorphism with disturbances of the catecholaminergic pathway that cause schizophrenia.[7]

Figure 11. (right) Mutated residue in juvenile L-DOPA responsive parkinsonism, Leu 206 (to Pro), is shown as a ball-and-stick model, and helix Cα2 is highlighted in pink. The active site α-helix Cα7 and Cα9 are highlighted in blue; Gly335 is colored green. The iron is colored red, and the iron-coordinating ligands are shown as ball-and-sticks. (left) View of the mutated residue that leads to L-DOPA responsive dystonia (Segawa's syndrome), Gln 382 (to Lys). The hydrogen bonds between Gln 382, Glu 251, and Arg 250 are shown in relation to the active site.

Examination of the $rTyrOH_{Cterm}$ structure has increased our understanding of neurological diseases caused by mutations in this enzyme. Missense point mutations in hTyrOH have been directly linked to the pathogenesis of juvenile L-DOPA responsive parkinsonism and L-DOPA responsive dystonia (Segawa's syndrome). These disorders are characterized by muscle rigidity caused in part by a dysfunction of dopaminergic neurons in the brainstem nuclei (basal ganglia) which are involved in the highest level of control of motoric functions as well as higher cognitive functions. The point mutation Leu205 (Leu206 in rTyrOH) to proline leads to a form of juvenile L-DOPA responsive parkinsonism.[5] The almost complete loss of enzyme activity associated with this mutation is attributed to a destabilization of the protein structure. This assessment is based on biochemical studies that found normal hTyrOH mRNA levels when transiently expressed in A293 cells but no TyrOH immunoreactivity.[5] In the crystal structure, Leu206 (in rTyrOH) is a solvent-exposed residue located at the midpoint of the α-helix Cα2, a 15 amino acid helix (Figure 11). This amphipathic helix lies on the surface of the protein and interacts with a 14 residue loop that connects the C-terminus of Cα2 to the α-helix Cα3 through a salt bridge (Arg203 to Glu229) and many hydrophobic contacts. Substitution of a proline within the α-helix may disrupt the helical packing of Cα2, which destabilizes the protein structure leading to improper folding of the enzyme and enhanced cytosolic proteolytic degradation. In this connection, it should be mentioned that hTyrOH has recently been shown to be a substrate for the ubiquitin conjugating enzyme system purified from rat liver cytosol (Døskeland and Flatmark, unpublished data) as previously shown for hPheOH.[46]

Another missense point mutation, Gln381 (Gln382 in rTyrOH) to Lys, causes a form of L-DOPA responsive dystonia (Segawa's syndrome).[4] The mutant TyrOH appears to be expressed at wild-type levels.[5] Biochemical studies have shown that the Q382K mutant exhibits 15% of wild-type specific activity and a lowered K_m value for tyrosine (6-fold for the recombinant *E. coli* protein), although the K_m for pterin and the levels of iron found in the protein appear to be relatively unaffected.[4] The residue Gln382 (in rTyrOH) is within a conserved strand on the protein surface located on the opposite side of the catalytic core from the entrance into the active site, 20 Å away from the iron (Figure 11). Hydrogen bonds are observed between the $N^{\epsilon 1}$ and $O^{\epsilon 2}$ from Gln382 to the main-chain amide group of Arg250 (Gly 249 in human TyrOH) and the side-chain oxygen of Glu251 (conserved in human TyrOH). These two residues lie in the first turn of helix Cα4. This α-helix directly contacts the α-helix Cα7, which lines the bottom of the active site. A lysine at position 382 would disrupt these interactions due to the longer side-chain length and the loss of a main-chain hydrogen bond. This might lead to a local movement in helix Cα4 and hence disturb the conformation of the active site. The reasons why this mutation only affects tyrosine binding (decreased affinity) cannot be addressed until the location of the substrate binding sites are determined.

5. Concluding Remarks

Substantial progress has been made in the past decade in elucidating the structure and function of the mammalian aromatic amino acid hydroxylases and some of their disease-related mutant forms. Notably, the recently emerging crystal structures of phenylalanine and tyrosine hydroxylase have shown a common three-domain organization of these enzymes, which provides an understanding of their oligomeric state and gives further insight into their catalytic and regulatory properties. Their catalytic

and tetramerization domains contain the same secondary structures in the same arrangement and with the same topological connections. The N-terminus of the regulatory domain in phenylalanine hydroxylase (not yet known for tyrosine hydroxylase), containing the single phosphorylation site, is positioned over the active site, while the majority of the regulatory domain packs against a symmetry-related neighboring catalytic domain. This organization most likely plays a critical role in the cooperative binding of the substrate (L-phenylalanine in phenylalanine hydroxylase), based on the similarities to other allosteric enzymes. A 13 Å channel appears to lead the way to the active site containing a five/six-coordinated iron (Fe(III) in the crystal structures) with two/three labile water molecules. The pterin cofactor is nonbonding to the iron atom with the pterin C4a atom about 5 Å away, in an ideal conformation for dioxygen to bind in a bridging position. Like many of the pterin-containing enzymes, the pterin cofactor in the aromatic amino acid hydroxylases π-stacks on an aromatic amino acid at the active site. In the case of tyrosine hydroxylase, a phenylalanine residue undergoes autohydroxylation in the *meta* position. The position of the reversible catechol inhibitors overlaps with the pterin cofactor binding site, and unlike amino acid substrate and cofactor, they bind directly to the iron atom in a bidentate coordination through the catechol hydroxyl groups, replacing two of the labile water molecules. One might speculate that the liganded iron atom has different conformational switches, including one to bind catechol inhibitor (in the Fe(III) form) and one to hydroxylate substrate (in the Fe(II) form). Thus, an unanswered question is whether there are changes in the iron ligation of the activated ferrous forms of the hydroxylases compared with their resting ferric forms. The crystallization of their binary complexes with the amino acid substrates and the ternary complexes also represents a challenge for future structural studies on these enzymes. The tetramerization domain uses a domain-swapping mechanism which allows for stability in the properly folded state, and mutations or chemical modifications in this region of the protein structure can lead to gross instability of the enzymes. The crystal structures have already been successfully used to understand the structural basis for the defect function of several disease-related mutant forms of the enzymes. This overall information now offers an unprecedented opportunity to design additional mutant forms which can more specifically contribute to answer the intriguing fundamental questions related to the catalytic mechanism, substrate specificity, and differences in regulatory properties between the aromatic amino acid hydroxylases, which are still poorly understood.

6. Acknowledgments

Our studies on the aromatic amino acid hydroxylases have been supported by the Research Council of Norway (T.F.), Rebergs legat (T.F.), the Novo Nordisk Foundation (T.F.), the European Commission (T.F.), and the Physical Biosciences Division of Lawrence Berkeley National Laboratory (R.C.S.). The work discussed here from our laboratories has been due in large part to the efforts of former and present co-workers, Drs. K. Goodwill, H. Erlandsen, F. Fusetti, C. Sabatier, A. P. Døskeland, J. Haavik, K. K. Andersson, A. Martinez, P. Knappskog, and B. Almås as well as E. Bjørgo, S. V. Berge, R. M. Svebak, and A. S. Munoz. We are indebted to our colleagues Profs. E. Hough and A. Muga.

7. Abbreviations and Definitions

BH_4	(6*R*)-L-*erythro*-5,6,7,8-tetrahydrobiopterin
BH_2	L-*erythro*-7,8-dihydrobiopterin
bTyrOH	bovine tyrosine hydroxylase
EPR	electron paramagnetic resonance
E/*D*	ratio of the rhombicity parameter (*E*) to zero-field splitting parameter (*D*) from the spin Hamiltonian equation. The ratio measures the deviation from axial electronic symmetry for a spin system with $S = {}^1/_2$. The EPR spectrum observed reflects the *E*/*D* ratio, and thus, it provides a convenient way to characterize and refer to different EPR-active species.
XAS	X-ray absorption
FT	Fourier transform
hPheOH	human phenylalanine hydroxylase
hTyrOH	human tyrosine hydroxylase
HPA	hyperphenylalaninemia
L-Phe	L-phenylalanine
L-Tyr	L-tyrosine
MCD	magnetic circular dichroism
NMR	nuclear magnetic resonance
PheOH	phenylalanine hydroxylase (EC 1.14.16.1)
PKU	phenylketonuria
rmsd	root-mean-square deviation
rPheOH	rat phenylalanine hydroxylase
rTyrOH	rat tyrosine hydroxylase
TyrOH	tyrosine hydroxylase (EC 1.14.16.2)
TrpOH	tryptophan hydroxylase (EC 1.14.16.4)

8. References

(1) Kappock, T. J.; Caradonna, J. B. *Chem. Rev.* **1996**, *96*, 2659−2756.
(2) Almås, B.; Haavik, J.; Flatmark, T. *Biochem. J.* **1996**, *319*, 947−951.
(3) Kaufman, S. *J. Biol. Chem.* **1959**, *234*, 2677−2682.
(4) Knappskog, P. M.; Flatmark, T.; Mallet, J.; Lüdecke, B.; Bartholome, K. *Hum. Mol. Genet.* **1995**, *4*, 1209−1212.
(5) Lüdecke, B.; Knappskog, P. M.; Clayton, P. T.; Surtees, R. A. H.; Clelland, J. D.; Heales, S. J. R.; Brand, M. P.; Bartholome, K.; Flatmark, T. *Hum. Mol. Genet.* **1996**, *5*, 1023−1028.
(6) Smyth, C.; Kalsi, G.; Curtis, D.; Brynjolfsson, J.; O'Neill, J.; Rifkin, L.; Moloney, E.; Murphy, P.; Petursson, H.; Gurling, H. *Genomics* **1997**, *39*, 271−278.
(7) Thibaut, F.; Ribeyre, J. M.; Dourmap, N.; Meloni, R.; Laurent, C.; Campion, D.; Menard, J. F.; Dollfus, S.; Mallet, J.; Petit, M. *Schizophr. Res.* **1997**, *23*, 259−264.
(8) Haavik, J.; Almås, B.; Flatmark, T. *J. Neurochem.* **1997**, *68*, 328−332.
(9) Hufton, S. E.; Jennings, I. G.; Cotton, R. G. H. *Biochem. J.* **1995**, *311*, 353−366.
(10) Goodwill, K. E.; Sabatier, C.; Marks, C.; Raag, R.; Fitzpatrick, P. F.; Stevens, R. C. *Nat. Struct. Biol.* **1997**, *4*, 578−585.
(11) Fusetti, F.; Erlandsen, H.; Flatmark, T.; Stevens, R. C. *J. Biol. Chem.* **1998**, *273*, 16962−16967.
(12) Erlandsen, H.; Fusetti, F.; Martinez, A.; Hough, E.; Flatmark, T.; Stevens, R. C. *Nat. Struct. Biol.* **1997**, *4*, 995−1000.
(13) Kobe, B.; Jennings, I. G.; House, C. M.; Michell, B. J.; Goodwill, K. E.; Santarsiero, B. D.; Stevens, R. C.; Cotton, R. G. H.; Kemp, B. E. *Nat. Struct. Biol.* **1998**, *6*, 1.
(14) Erlandsen, H.; Flatmark, T.; Stevens, R. C.; Hough, E. *Biochemistry* **1998**, *37*, 15638−15646.
(15) Goodwill, K. E.; Sabatier, C.; Stevens, R. C. *Biochemistry* **1998**, *37*, 13437−13445.
(16) Kaufman, S. *Adv. Enzymol. Relat. Areas Mol. Biol.* **1993**, *67*, 77−264.

(17) Knappskog, P. M.; Flatmark, T.; Aarden, J. M.; Haavik, J.; Martinez, A. *Eur. J. Biochem.* **1996**, *242*, 813−821.
(18) Martinez, A.; Andersson, K. K.; Haavik, J.; Flatmark, T. *Eur. J. Biochem.* **1991**, *198*, 675−682.
(19) Gibbs, B. S.; Wojchowski, D.; Benkovic, S. J. *J. Biol. Chem.* **1993**, *268*, 8046−8052.
(20) Martinez, A.; Olafsdottir, S.; Flatmark, T. *Eur. J. Biochem.* **1993**, *211*, 259−266.
(21) Meyer-Klaucke, W.; Winkler, H.; Schunemann, V.; Trautwein, A. X.; Nolting, H. F.; Haavik, J. *Eur. J. Biochem.* **1996**, *241*, 432−439.
(22) Jennings, I. G.; Kemp, B. E.; Cotton, R. G. H. *Proc. Natl. Acad. Sci. U.S.A.* **1991**, *88*, 5734−5738.
(23) Martinez, A.; Vageli, O.; Pfleiderer, W.; Flatmark, T. *Pteridines* **1998**, *9*, 44−52.
(24) Ayling, J. E.; Boehm, G. R.; Textor, S. C.; Pirson, R. A. *Biochemistry* **1973**, *12*, 2045−2051.
(25) Bailey, S. W.; Dillard, S. B.; Thomas, K. B.; Ayling, J. E. *Biochemistry* **1989**, *28*, 494−504.
(26) Almås, B.; Le Bourdelles, B.; Flatmark, T.; Mallet, J.; Haavik, J. *Eur. J. Biochem.* **1992**, *209*, 249−255.
(27) Martinez, A.; Haavik, J.; Flatmark, T. *Eur. J. Biochem.* **1990**, *193*, 211−219.
(28) Han, S.; Eltis, L. D.; Timmis, K. N.; Muchmore, S. W.; Bolin, J. T. *Science* **1995**, *270*, 976−980.
(29) Hegg, E. L.; Que, L. *Eur. J. Biochem.* **1997**, *250*, 625−629.
(30) Martinez, A.; Abeygunawardana, C.; Haavik, J.; Flatmark, T.; Mildvan, A. S. *Biochemistry* **1993**, *32*, 6381−6390.
(31) Fitzpatrick, P. F. *Biochemistry* **1991**, *30*, 3658−3662.
(32) Fitzpatrick, P. F. *Biochemistry* **1991**, *30*, 6386-6391.
(33) Andersson, K. K.; Cox, D. D.; Que, L., Jr.; Flatmark, T.; Haavik, J. *J. Biol. Chem.* **1988**, *263*, 18621−18626.
(34) Haavik, J.; Martinez, A.; Flatmark, T. *FEBS Lett.* **1990**, *262*, 363−365.
(35) (a) Haavik, J.; Martinez, A.; Olafsdottir, S.; Mallet, J.; Flatmark, T. *Eur. J. Biochem.* **1992**, *210*, 23−31. (b) Miller, M.; Shiman, R. *J. Biol. Chem.* **1976**, *251*, 3671−3676.
(36) Døskeland, A. P.; Ljones, T.; Skotland, T.; Flatmark, T. *Neurochem. Res.* **1982**, *7*, 407−421.
(37) Parniak, M. A. In *Unconjugated pterins and related biogenic amines*; Curtius, H. C., Blau, N., Eds; Walter de Gruyter & Co: Berlin, 1987.
(38) Martinez, A.; Knappskog, P. M.; Olafsdottir, S.; Døskeland, A. P.; Eiken, H. G.; Svebak, R. M.; Bozzini, M. L.; Apold, J.; Flatmark, T. *Biochem. J.* **1995**, *306*, 589−597.
(39) Kappock, T. J.; Harkins, P. C.; Friedenberg, S.; Caradonna, J. P. *J. Biol. Chem.* **1995**, *270*, 30532−30544.
(40) Vrana, K. E.; Walker, S. J.; Rucker, P.; Liu, X. *J. Neurochem.* **1994**, *63*, 2014−2020.
(41) Shiman, R.; Gray, D. W.; Pater, A. *J. Biol. Chem.* **1979**, *254*, 11300−11306.
(42) Døskeland, A. P.; Døskeland, S. O.; Øgreid, D.; Flatmark, T. *J. Biol. Chem.* **1984**, *259*, 11242−11248.
(43) Phillips, R. S.; Parniak, M. A.; Kaufman, S. *Biochemistry* **1984**, *23*, 3836−3842.
(44) Chehin, R.; Thorolfsson, M.; Knappskog, P. M.; Martinez, A.; Flatmark, T.; Arrondo, J. L. R.; Muga, A. *FEBS Lett.* **1998**, *422*, 225−230.
(45) Davis, M. D.; Parniak, M. A.; Kaufman, S.; Kempner, E. *Proc. Natl. Acad. Sci. U.S.A.* **1997**, *94*, 491−495.
(46) Døskeland, A. P.; Flatmark, T. *Biochem. J.* **1996**, *319*, 941−945.
(47) Grant, G. A.; Schuller, D. J.; Banaszak, L. J. *Protein Sci.* **1996**, *5*, 34−41.
(48) Stevens, R. C.; Gouaux, J. E.; Lipscomb, W. N. *Biochemistry* **1990**, *29*, 7691−7701.
(49) Shiman, R.; Gray, D. W. *J. Biol. Chem.* **1980**, *255*, 4793−4800.
(50) Frieden, C. *Annu. Rev. Biochem.* **1979**, *48*, 471−489.
(51) Shiman, R. *J. Biol. Chem.* **1980**, *255*, 10029−10032.
(52) Mitnaul, L. J.; Shiman, R. *Proc. Natl. Acad. Sci. U.S.A.* **1995**, *92*, 885−889.
(53) Cronk, J. D.; Endrizzi, J. A.; Alber, T. *Protein Sci.* **1996**, *5*, 1963−1972.
(54) Døskeland, A. P.; Schworer, C. M.; Døskeland, S. O.; Chrisman, T. D.; Soderling, T. R.; Corbin, J. D.; Flatmark, T. *Eur. J. Biochem.* **1984**, *145*, 31−37.
(55) Chen, R.; Grobler, J. A.; Hurley, J. H.; Dean, A. M. *Protein Sci.* **1996**, *5*, 287−295.
(56) Russo, A. A.; Jeffrey, P. D.; Pavletich, N. P. *Nat. Struct. Biol.* **1996**, *3*, 696−700.
(57) Barford, D.; Johnson, L. N. *Nature* **1989**, *340*, 609−616.
(58) Milstien, S.; Abita, J. P.; Chang, N.; Kaufman, S. *Proc. Natl. Acad. Sci. U.S.A.* **1976**, *73*, 1591−1593.
(59) Døskeland, A. P.; Martinez, A.; Knappskog, P. M.; Flatmark, T. *Biochem. J.* **1996**, *313*, 409−414.
(60) Kobe, B.; Jennings, I. G.; House, C. M.; Feil, S. C.; Michell, B. J.; Tiganis, T.; Parker, M. W.; Cotton, R. G.; Kemp, B. E. *Protein Sci.* **1997**, *6*, 1352−1357.
(61) Daubner, S. C.; Hillas, P. J.; Fitzpatrick, P. F. *Biochemistry* **1997**, *36*, 11574−11582.
(62) Quinsey, N. S.; Lenaghan, C. M.; Dickson, P. W. *J. Neurochem.* **1996**, *66*, 908−914.
(63) McTigue, M. A.; Davies, J. F.; Kaufman, B. T.; Kraut, J. *Biochemistry* **1992**, *31*, 7264−7273.
(64) Crane, B. R.; Arvai, A. S.; Ghosh, D. K.; Wu, C.; Getzoff, E. D.; Stuehr, D. J.; Tainer, J. A. *Science* **1998**, *279*, 2121−2126.
(65) Kaufman, S. *Adv. Enzymol. Relat. Areas Mol. Biol.* **1995**, *70*, 103−220.
(66) Kaufman, S. *J. Biol. Chem.* **1979**, *254*, 5150−5154.
(67) Kaufman, S. *J. Biol. Chem.* **1964**, *239*, 332−338.
(68) Gibbs, B. S.; Benkovic, S. J. *Biochemistry* **1991**, *30*, 6795−6802.
(69) Dickson, P. W.; Jennings, I. G.; Cotton, R. G. H. *J. Biol. Chem.* **1994**, *269*, 20369−20375.
(70) Nixon, J. C. In *Folates and Pterins*; Blakley, R. L., Benkovic, S. J., Eds; John Wiley & Sons: New York, 1985.
(71) Vasudevan, S. G.; Shaw, D. C.; Armarego, W. L. *Biochem. J.* **1988**, *255*, 581−588.
(72) Fukami, M. H.; Haavik, J.; Flatmark, T. *Biochem. J.* **1990**, *268*, 525−528.
(73) Francisco, W. A.; Tian, G.; Fitzpatrick, P. F.; Klinman, J. P. *J. Am. Chem. Soc.* **1998**, *120*, 4057−4062.
(74) Dix, T. A.; Kuhn, D. M.; Benkovic, S. J. *Biochemistry* **1987**, *26*, 3354−3361.
(75) Hillas, P. J.; Fitzpatrick, P. F. *Biochemistry* **1996**, *35*, 6968−6975.
(76) Dix, T. A.; Bollag, G. E.; Domanico, P. L.; Benkovic, S. J. *Biochemistry* **1985**, *24*, 2955−2958.
(77) Massey, V.; Hemmerich, P. In *The Enzymes 12*; Boyer, P. D., Ed.; Academic Press: New York, 1975.
(78) (a) Massey, V. *J. Biol. Chem.* **1994**, *269*, 22459−22462. (b) Flatmark, T.; Almas, B.; Knappskog, P. M.; Berge, S. V.; Svebak, R. M.; Chehin, R.; Muga, A.; Martinez, A. *Eur. J. Biochem.* **1999**, in press.
(79) Liu, X.; Vrana, K. E. *Neurochem. Int.* **1991**, *1*, 27−31.
(80) Daubner, S. C.; Lohse, D. L.; Fitzpatrick, P. F. *Protein Sci.* **1993**, *2*, 1452−1460.
(81) Garrod, A. E. In *Inborn Errors of Metabolism*, 2nd ed.; Henry Frowde and Hodder & Stoughton: London, 1923.
(82) Følling, A.; Hoppe-Seyler's, Z. *Physiol. Chem.***1934**, *227*, 169−176.
(83) Reynolds, R.; Burri, R.; Herschkowitz, N. *Exp. Neurol.* **1993**, *124*, 357−367.
(84) Nowacki, P. M.; Byck, S.; Prevost, L.; Scriver, C. R. *Nucleic Acids Res.* **1998**, *26*, 220−225.
(85) Flatmark, T.; Knappskog, P. M.; Bjørgo, E.; Martinez, A. In *Chemistry and Biology of Pteridines and Folates 1997*; Pfleiderer, W., Rokos, H., Eds.; Blackwell Science: Berlin, 1997; pp 503−508.
(86) Baric, L.; Mardesic, D.; Sarnavoka, V.; Lichter-Konecki, U.; Konecki, D. S.; Trefz, F. K. *J. Inherited Metab. Dis.* **1994**, *17*, 376−377.
(87) Okano, Y.; Wang, T.; Eisensmith, R. C.; Longhi, R.; Riva, E.; Giovannini, M.; Cerone, R.; Romano, C.; Woo, S. L. C. *Genomics* **1991**, *9*, 96−103.
(88) Knappskog, P. M.; Eiken, H. G.; Martinez, A.; Olafsdottir, S.; Haavik, J.; Flatmark, T.; Apold, J. *Adv. Exp. Med. Biol.* **1993**, *338*, 59−62.
(89) Bjørgo, E.; Knappskog, P. M.; Martinez, A.; Stevens, R. C.; Flatmark, T. *Eur. J. Biochem.* **1998**, *257*, 1−10.
(90) Di Lella, A. G.; Marvit, J.; Lidsky, A. S.; Guttler, F.; Woo, S. L. C. *Nature* **1986**, *322*, 799−803.
(91) DiLella, A. G.; Marvit, J.; Brayton, K.; Woo, S. L. C. *Nature* **1987**, *327*, 333−336.
(92) Lichter-Konecki, U.; Konecki, D. S.; DiLella, A. G.; Brayton, K.; Marvit, J.; Hahn, T. M.; Trefz, F. K.; Woo, S. L. C. *Biochemistry* **1988**, *27*, 2881−2885.
(93) Wang, T.; Okano, Y.; Eisensmith, R. C.; Harvey, M. L.; Lo, W. H. Y.; Huang, S.-Z.; Zeng, Y.-T.; Yuan, L.-F.; Furuyama, J.-I.; Oura, T.; Sommer, S. S.; Woo, S. L. C. *Proc. Natl. Acad. Sci. U.S.A.* **1991**, *88* , 2146−2150.
(94) Nar, H.; Huber, R.; Auerbach, G.; Fischer, M.; Hösl, C.; Ritz, H.; Bracher, A.; Meining, W.; Eberhardt, S.; Bacher, A. *Proc. Natl. Acad. Sci. U.S.A.* **1995**, *92*, 12120−12125.
(95) Nichol, C. A.; Smith, G. K.; Duch, D. S. *Annu. Rev. Biochem.* **1985**, *54*, 729−764.
(96) Auerbach, G.; Herrmann, A.; Gütlich, M.; Fischer, M.; Jacob, U.; Bacher, A.; Huber, R. *Pteridines* **1997**, *8*, 61−62.
(97) Nar, H.; Huber, R.; Heizmann, C. W.; Thöny, B.; Bürgisser, D. *EMBO J.* **1994**, *13*, 1255−1262.
(98) Kabsch, W.; Sander, C. *Biopolymers* **1983**, *22*, 2577−2637.
(99) Kraulis, P. J. *J. Appl. Crystallogr.* **1991**, *24*, 946−950.
(100) Meritt, E. A.; Murphy, M. E. P. *Acta Crystallogr. D* **1994**, *50*, 869−873.
(101) Varughese, K. I.; Skinner, M. M.; Whiteley, J. M.; Matthews, J. A.; Xuong, N. H. *Proc. Natl. Acad. Sci. U.S.A.* **1992**, *89*, 6080−6085.

CR980450Y